
















KARRIKIN INSENSITIVE2 regulates leaf development, root system architecture and arbuscular-mycorrhizal symbiosis in *Brachypodium distachyon*

Yongjie Meng^{1,2,†} , Kartikye Varshney^{3,†} , Norbert Incze^{4,5} , Eszter Badics^{4,5} , Muhammad Kamran¹ , Sabrina F. Davies¹ , Larissa M. F. Oppermann¹, Kévin Magne^{6,7} , Marion Dalmais^{6,7} , Abdel Bendahmane^{6,7} , Richard Sibout^{8,9} , John Vogel¹⁰ , Debbie Laudencia-Chingcuanco¹¹ , Charles S. Bond¹, Vilmos Soós⁴ , Caroline Gutjahr^{3,*}  and Mark T. Waters^{1,2,*} 

¹School of Molecular Sciences, The University of Western Australia, Perth, WA 6009, Australia,

²College of Agronomy, Sichuan Agricultural University, Chengdu 611130, China,

³Plant Genetics, TUM School of Life Sciences, Technical University of Munich, Freising 85354, Germany,

⁴Department of Biological Resources, Agricultural Institute, Centre for Agricultural Research, Martonvásár 2462, Hungary,

⁵Doctoral School of Biology, Institute of Biology, ELTE Eötvös Loránd University, Budapest 1117, Hungary,

⁶Université Paris-Saclay, CNRS, INRAE, Univ Evry, Institute of Plant Sciences Paris-Saclay (IPS2), Orsay 91405, France,

⁷Université de Paris, CNRS, INRAE, Institute of Plant Sciences Paris-Saclay (IPS2), Orsay 91405, France,

⁸Institut Jean-Pierre Bourgin, UMR1318 INRAE-AgroParisTech, Versailles Cedex F-78026, France,

⁹UR1268 BIA, INRAE, Nantes 44300, France,

¹⁰DOE Joint Genome Institute, Berkeley, California 94720, USA, and

¹¹USDA-Agricultural Research Service, Western Regional Research Center, Albany, California 94710, USA

Received 26 August 2021; accepted 20 December 2021; published online 25 December 2021.

*For correspondence (e-mail mark.waters@uwa.edu.au; caroline.gutjahr@tum.de).

†These authors are contributed equally.

SUMMARY

KARRIKIN INSENSITIVE2 (KAI2) is an α/β -hydrolase required for plant responses to karrikins, which are abiotic butenolides that can influence seed germination and seedling growth. Although represented by four angiosperm species, loss-of-function *kai2* mutants are phenotypically inconsistent and incompletely characterised, resulting in uncertainties about the core functions of KAI2 in plant development. Here we characterised the developmental functions of KAI2 in the grass *Brachypodium distachyon* using molecular, physiological and biochemical approaches. *Bdkai2* mutants exhibit increased internode elongation and reduced leaf chlorophyll levels, but only a modest increase in water loss from detached leaves. *Bdkai2* shows increased numbers of lateral roots and reduced root hair growth, and fails to support normal root colonisation by arbuscular-mycorrhizal (AM) fungi. The karrikins KAR₁ and KAR₂, and the strigolactone (SL) analogue *rac*-GR24, each elicit overlapping but distinct changes to the shoot transcriptome via BdKAI2. Finally, we show that BdKAI2 exhibits a clear ligand preference for desmethyl butenolides and weak responses to methyl-substituted SL analogues such as GR24. Our findings suggest that KAI2 has multiple roles in shoot development, root system development and transcriptional regulation in grasses. Although KAI2-dependent AM symbiosis is likely conserved within monocots, the magnitude of the effect of KAI2 on water relations may vary across angiosperms.

Keywords: α/β -hydrolase, arbuscular-mycorrhiza, butenolide, *Brachypodium distachyon*, karrikin, symbiosis, strigolactone.

INTRODUCTION

Karrikins, of which KAR₁ and KAR₂ are representatives, are a class of abiotic plant growth regulators produced from the partial combustion of plant material (Flematti et al., 2004; Flematti et al., 2009). Released into the soil following wildfires, karrikins can promote seed germination

and seedling photomorphogenesis, and thereby facilitate the revegetation process (Nelson et al., 2009, 2010; Stevens et al., 2007). The butenolide moiety of karrikins is also an essential structural feature of strigolactones (SLs), which are carotenoid-derived plant hormones that regulate a range of developmental processes in plants, and also

serve as a rhizosphere signal for arbuscular-mycorrhizal (AM) fungi and root parasitic weeds (Waters et al., 2017; Bürger and Chory, 2020). Collectively, these butenolides possess wide-ranging biological activities with considerable agricultural and environmental significance.

Consistent with their chemical similarity, the signal transduction pathways for karrikins and SLs are broadly homologous. The α/β -hydrolase KARRIKIN INSENSITIVE2 (KAI2; also known as DWARF14-LIKE and HYPOSENSITIVE TO LIGHT) is the likely karrikin receptor (Waters et al., 2012; Guo et al., 2013; Lee et al., 2018; Sun et al., 2020), while a paralogous α/β -hydrolase DWARF14 (D14) serves as the SL receptor (Hamiaux et al., 2012; de Saint Germain et al., 2016; Yao et al., 2016; Shabek et al., 2018). Both karrikins and SLs act through the F-box protein MAX2 (MORE AXILLARY BRANCHES2), which targets members of the SMXL (SUPPRESSOR-OF-MAX2-1-LIKE) family of repressor proteins for polyubiquitination and subsequent proteasomal degradation (Nelson et al., 2011; Stanga et al., 2013; Zhou et al., 2013; Jiang et al., 2013; Zhao et al., 2015). Specificity in karrikin and SL response arises both from intrinsic differences in ligand preference between KAI2 and D14 (Scaffidi et al., 2014; Wang et al., 2020; Arellano-Saab et al., 2021; Yao et al., 2021), and through degradation of specific SMXL proteins that associate with each receptor upon ligand recognition (Soundappan et al., 2015; Wang et al., 2015, 2020; de Saint Germain et al., 2016; Khosla et al., 2020; Zheng et al., 2020). The similar componentry of KAI2- and D14-dependent signalling, the evolutionary conservation of KAI2, and the fact that *kai2* phenotypes are opposite to the effects of applying karrikins, collectively have led to the proposal that KAI2 is a receptor for an endogenous butenolide compound(s) called 'KAI2 ligand' (KL; Nelson et al., 2011; Conn and Nelson, 2016; Sun et al., 2016; Yao et al., 2021). From this viewpoint, karrikins are KAI2 agonists that mimic KL, or otherwise enhance KL activity.

Numerous roles for KL in plant development have been inferred from *kai2* mutant phenotypes of *Arabidopsis*, *Lotus japonicus* and *Petunia hybrida*. These include regulation of seed germination (Waters et al., 2012), hypocotyl and cotyledon growth (Sun and Ni 2011; Waters et al., 2012), leaf and petiole elongation (Waters et al., 2012, 2015b; Soundappan et al., 2015; Bennett et al., 2016), hypodermal passage cell number (Liu et al., 2019), root system architecture and root hair growth (Villaécija-Aguilar et al., 2019; Carbonnel et al., 2020b; Swarbreck et al., 2020), root skewing (Swarbreck et al., 2019; Villaécija-Aguilar et al., 2019), and the regulation of leaf cuticle development and stomatal aperture (Li et al., 2017). In *Arabidopsis*, *kai2* mutants are hypersensitive to water deficit (Li et al., 2017), which implies that KL signalling might promote drought tolerance.

A further prominent role for KL signalling via KAI2 was revealed through screens for mutants defective in the symbiotic colonisation of plant roots by AM fungi. The fungus

assists the plant with the acquisition of inorganic phosphate and nitrogen, in exchange for carbohydrates and lipids (Smith and Smith, 2011; Roth and Paszkowski, 2017; Keymer and Gutjahr, 2018). In rice, loss of KAI2 function almost entirely abolishes root colonisation, and also results in a failure of rice roots to initiate transcriptional responses to fungal exudates, suggesting that KAI2-dependent signalling is involved in initial steps in the symbiotic process (Gutjahr et al., 2015; Choi et al., 2020). A similar requirement for KAI2 in AM symbiosis has been inferred in petunia (Liu et al., 2019), suggesting that this may be a widespread and conserved function for KAI2. However, several traits ascribed to KAI2 are inconsistent between species: for example, loss of KAI2 does not impair hypocotyl growth or affect root hair length in *L. japonicus*, while both traits are impacted in *Arabidopsis* (Villaécija-Aguilar et al., 2019; Carbonnel et al., 2020b). A role for KAI2 in AM symbiosis has not been established beyond rice and *Petunia*, nor has drought tolerance been investigated beyond *Arabidopsis*. Developmental and stress-related *kai2* phenotypes have not been described in monocots, except for increased mesocotyl elongation in rice (Gutjahr et al., 2015; Zheng et al., 2020). Our understanding of KAI2-dependent signalling, and thus the applicability of this knowledge for crop improvement, is limited to the few species in which KAI2 function has been investigated, among which monocots are under-represented.

Brachypodium distachyon (hereafter 'Brachypodium') is a diploid grass that is a tractable model for cereal crops as well as perennial bioenergy crops with more complex genetics (Brutnell et al., 2012; Girin et al., 2014). A sequenced genome, germplasm resources and transformation procedures have all contributed to the development of this species as a model system (The International Brachypodium Initiative, 2010; Mur et al., 2011). Brachypodium symbioses have been reported with five species of AM fungi from two genera (Hong et al., 2012). As such, we recognised Brachypodium as an ideal system for expanding our knowledge of the functional basis of KAI2 signalling in plant development. Here we characterised two *Bdkai2* mutant alleles at the phenotypic, transcriptomic and molecular levels. We found a clear requirement for BdKAI2 in the establishment of AM symbiosis, root system architecture and shoot development, which is consistent with a broadly conserved role for KAI2-dependent signalling in angiosperm development.

RESULTS

BdKAI2 functions in shoot and leaf development

We screened for mutations in the homologue of KAI2 in Brachypodium (*BdKAI2*; Bradi1g15880). Two missense alleles, *Bdkai2-1* and *Bdkai2-2*, were identified from separate sodium azide-mutagenised populations in the Bd21-3

background. *Bdkai2-1* was identified via a TILLING screen, while *Bdkai2-2* resulted from a bulk sequencing screen (Figure S1; Methods S1). Each mutation was predicted to affect a highly conserved glycine residue (G54 or G56)

located in a loop region shortly after $\beta 4$ of the core domain of canonical α/β -fold hydrolases (Figures 1a,b and S2). Both mutations resulted in a non-conservative substitution to aspartic acid, and both were predicted to be deleterious

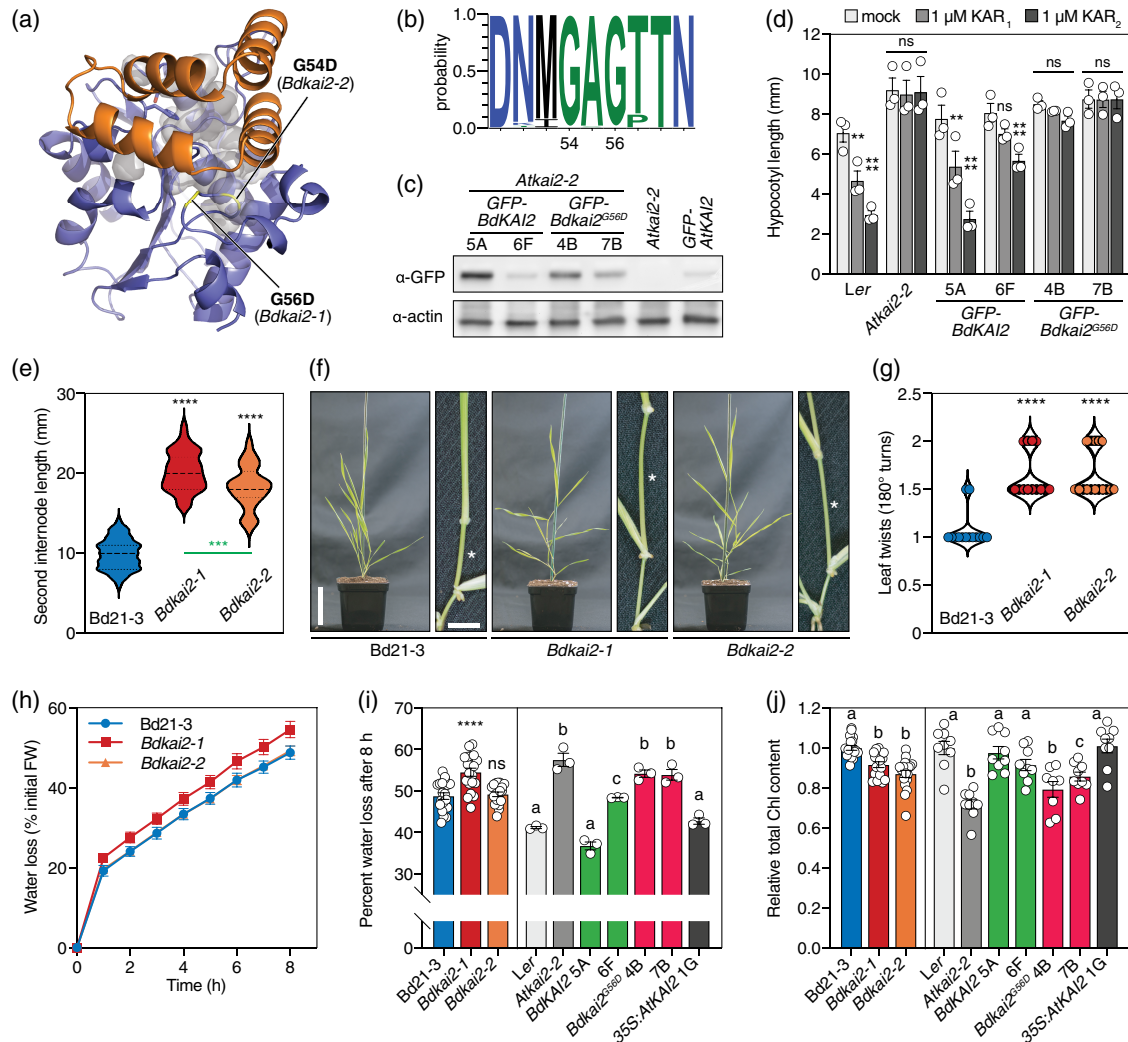


Figure 1. KAI2 has multiple functions in shoot development in *Brachypodium distachyon*. (a) Predicted homology model of BdkAI2 and the location of glycine 56 and glycine 54 residues mutated to aspartic acid in *Bdkai2-1* and *Bdkai2-2*, respectively. The four helices of the lid domain are highlighted in orange, the core domain in blue, and internal cavities are shown as transparent grey surface. Model was built using PDB 5z7w as a template. (b) Sequence logo derived from 476 angiosperm KAI2 homologues to show conservation at positions 54 and 56. (c) Immunoblot analysis of soluble protein extracts from two homozygous lines of *Arabidopsis thaliana* seedlings expressing either *AtKAI2pro::GFP-BdKAI2* or *GFP-Bdkai2-1* (G56D) transgenes in the *Atkai2-2* (*Ler*) background. An *AtKAI2pro::GFP-AtKAI2* extract serves as a positive control. (d) Hypocotyl elongation response of *Arabidopsis* transgenic seedlings described in (c) to karrikins. Seedlings were grown in the presence of 1 μ M KAR₁, KAR₂ or an equivalent volume of acetone for 4 days. Data are means \pm SE of $n = 3$ experimental replicates performed on separate occasions, with each replicate consisting of >20 individual seedlings per treatment. Asterisks indicate a significant difference from mock-treated seedlings: ** $P < 0.01$; **** $P < 0.0001$ (two-way ANOVA with Dunnett's multiple comparisons test). (e) Length of the second internode in *Brachypodium kai2* mutants. Dashed lines: median; dotted lines: quartiles; $n = 38$ –58 plants. Black asterisks indicate a significant difference relative to Bd21-3; green asterisks denote a significant difference between *Bdkai2-1* and *Bdkai2-2*; **** $P < 0.0001$; **** $P < 0.0001$ (one-way ANOVA). (f) Representative images of *Bdkai2* mutants at 4 weeks post-germination. Second internodes are indicated with asterisks. Scale bars: 50 mm and 5 mm. (g) Quantification of twisting in the second leaf of *Bdkai2*. ****Indicates a significant difference from Bd21-3 ($P < 0.0001$; Kruskal–Wallis; $n > 14$ seedlings per genotype). (h) Rate of water loss from *Bdkai2* shoots as a percentage of initial shoot weight following detachment from roots. Data are means \pm 95% CI of $n = 18$ –20 plants per genotype, combined from two independent experiments each consisting of 8–10 plants per genotype. (i) Comparison of water loss from shoots of *Bdkai2* (left) and complemented *Arabidopsis* lines (right) 8 h after detachment from roots. Data are means \pm SE of $n = 18$ –20 plants per genotype for *Brachypodium*, and $n = 3$ plants for *Arabidopsis*. ****Indicates a significant difference from Bd21-3 ($P < 0.0001$); ns, not significant (one-way ANOVA). For *Arabidopsis* data, (a–c) indicate different significance groupings (one-way ANOVA, $\alpha = 0.05$). (j) Chlorophyll content of the same genotypes as in (i). Data are expressed relative to the average total Chl content for the respective WT (Bd21-3 or *Ler*). Different lowercase letters indicate different significance groupings (one-way ANOVA, $\alpha = 0.05$). Statistical analysis was performed separately for data from *Brachypodium* ($n = 18$ plants per genotype) and *Arabidopsis* ($n = 9$ plants per genotype).

by PROVEAN (Choi and Chan, 2015) and Meta-SNP (Capriotti et al., 2013; Table S2).

To determine if BdKAI2 is functionally orthologous to Arabidopsis KAI2, and to verify that the *Bdkai2-1* mutation results in a non-functional protein, we transgenically complemented the Arabidopsis *Atkai2-2* mutant by expressing either BdKAI2 or Bdkai2^{G56D} as green fluorescent protein (GFP) fusion proteins. The N-terminal GFP serves as a tag for immunoblotting and does not affect KAI2 function (Sun et al., 2020). Both were controlled by the *AtKAI2* promoter and 5'UTR to achieve an expression profile native to Arabidopsis. We characterised homozygous lines expressing each fusion protein: two lines expressing GFP-BdKAI2 either at relatively high (5A) or low (6F) levels, while GFP-Bdkai2^{G56D} accumulated at moderate levels in both lines 4B and 7B (Figure 1c). Thus, both protein variants were stable in plant tissue, even though many missense mutations destabilise KAI2 (Yao et al., 2018; Sun et al., 2020).

Although the magnitude correlated with expression level, *GFP-BdKAI2* transgenics complemented the long hypocotyl phenotype and karrikin insensitivity of *Atkai2-2*, and exhibited a stronger hypocotyl response to KAR₂ than to KAR₁ (Figure 1d). Both lines expressing GFP-Bdkai2^{G56D} were insensitive to karrikins. We also examined seed germination and leaf morphology in these transgenics, and found that expression of the wild-type GFP-BdKAI2 protein, but not GFP-Bdkai2^{G56D}, restored these developmental deficiencies of *Atkai2-2* (Figure S3). From these data, we conclude that BdKAI2 is the functional orthologue of AtKAI2, that BdKAI2 shows preference for KAR₂ over KAR₁, and that the G56D mutation in *Bdkai2-1* renders the protein non-functional at various phenotypic levels.

In Brachypodium itself, *Bdkai2-1* and *Bdkai2-2* both conferred an elongated appearance to juvenile plants, exemplified by substantially longer internodes than Bd21-3. This phenotype was more pronounced in *Bdkai2-1* than *Bdkai2-2*, which may reflect a difference in allelic strength (Figure 1e,f). Leaf blades were frequently more twisted (Figure 1f,g) in both mutant alleles, suggesting that BdKAI2 might influence leaf morphology and development as it does in Arabidopsis, although with a different morphological outcome (Figure S3). We also examined whether leaf blades of *Bdkai2* mutants lose water faster than the wild-type, as has been reported for *Atkai2* (Li et al., 2017). Surprisingly, detached shoots of *Bdkai2-1*, but not *Bdkai2-2*, lost water only slightly faster than wild-type; on average, *Bdkai2-1* lost about 12% more water than Bd21-3 over 8 h (Figure 1h,i). In contrast, *Atkai2-2* lost about 40% more water than *Ler* over the same time period (Figure 1i). Expression of GFP-BdKAI2 was able to complement this defect in Arabidopsis, albeit to an extent that depended on expression strength, whereas GFP-Bdkai2^{G56D} was ineffective (Figure 1i). Finally, we observed that the leaves of both *Bdkai2* alleles were slightly pale green, and contained

~10% less total chlorophyll than wild-type (Figure 1j). Likewise, *Atkai2* leaves contained ~30% less total chlorophyll than *Ler*, and this defect was restored by expression of GFP-BdKAI2 but not GFP-Bdkai2^{G56D} (Figure 1j). Overall, these results demonstrate that loss of KAI2 function in Brachypodium leads to deficiencies in shoot development that are broadly consistent with mutant phenotypes observed in Arabidopsis. However, the contribution of KAI2 towards the control of water loss is relatively minor, because it is only detectable in the stronger *Bdkai2-1* allele.

Loss of BdKAI2 results in abnormal root system architecture

Relative to Bd21-3, both *Bdkai2* alleles conferred a dramatic increase in lateral root count (Figure 2a–d). On the primary root, the distance from the quiescent centre to the region of root hair emergence was substantially increased in *Bdkai2*, and root hair length was about half that of Bd21-3 throughout the root hair elongation zone (Figure 2e–i). Overall root hair density – here a combined measure of root hair length and count – was similarly reduced in *Bdkai2* (Figure 2j). Interestingly, *Bdkai2-1* exhibited a more severe root hair development phenotype than *Bdkai2-2*, again suggesting that the two alleles show some difference in strength, or that unidentified secondary mutations also impact upon this particular phenotype. *GFP-BdKAI2* restored the defective root hair length and root hair density phenotypes of *Atkai2-2* in transgenic Arabidopsis, whereas *GFP-Bdkai2^{G56D}* did not (Figure S4). These results demonstrate that the roles of KAI2-dependent signalling in lateral root and root hair development are conserved across monocots and dicots.

BdKAI2 is essential for AM symbiosis

We next examined the capacity of *Bdkai2* roots to support AM symbiosis. We found that both *Bdkai2-1* and *Bdkai2-2* were not colonised by the AM fungus *Rhizophagus irregularis* (Figure 3a–c). Although hyphae were present on the root surface, the mutants were largely unable to support the complete development of hyphopodia, internal hyphae, arbuscules or vesicles (Figure 3d). Overall, less than 10% of the root length was colonised in *Bdkai2*, compared with about 60% in Bd21-3. In the very rare cases in which the fungus entered the root, fully developed arbuscules were formed.

We also quantified levels of two AM-associated marker transcripts *BdAM43* and *BdPT7* (Hong et al., 2012). Both were strongly induced in Bd21-3 following inoculation with *R. irregularis* (~28- and ~250-fold for *BdAM43* and *BdPT7*, respectively), but these responses were substantially reduced in *Bdkai2* mutants (Figure 3e,f). Indeed, *Bdkai2-1* – which has more severe root hair and internode length phenotypes – showed no significant difference in *BdAM43* or *BdPT7* transcript levels following spore inoculation. *DLK2*, a paralogue of *D14* and *KAI2*, is considered to be the best

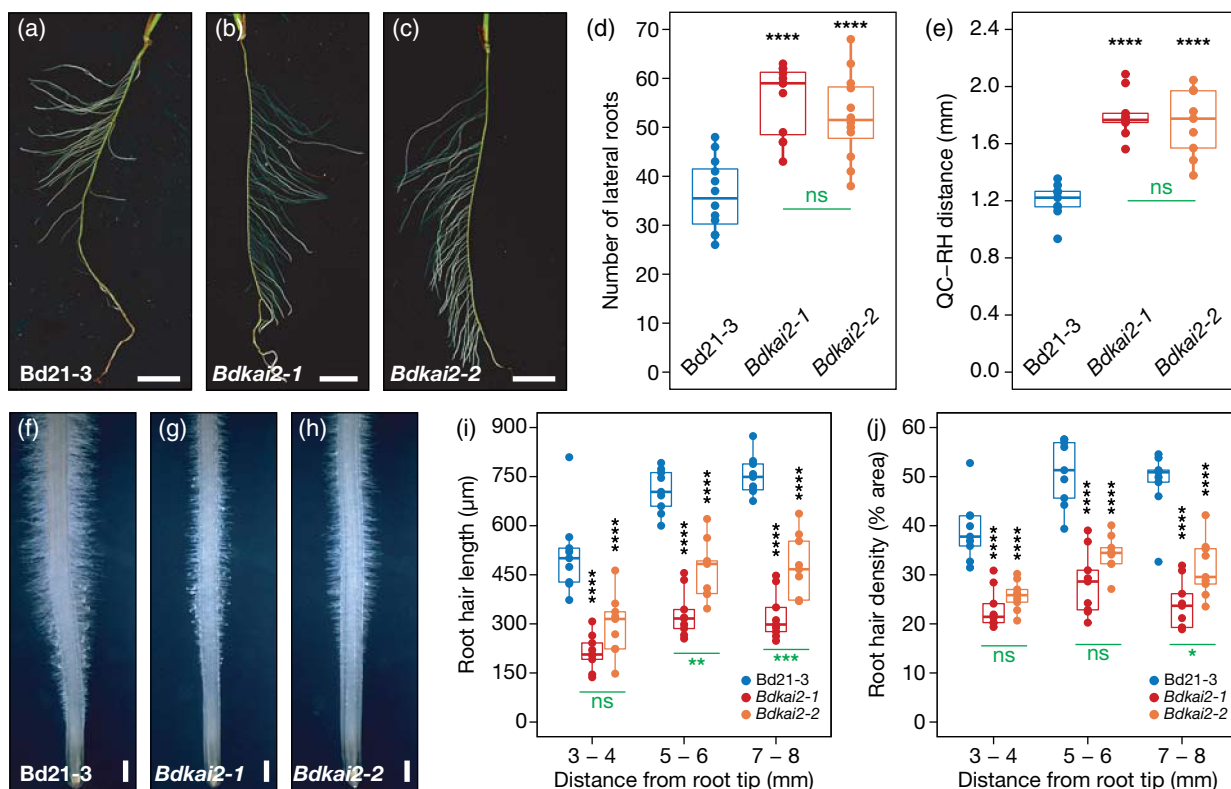


Figure 2. KAI2 is required for normal root development in *Brachypodium distachyon*. (a–c) Representative images of the root system of 17-day-old wild-type (Bd21-3) and *Bdkai2* seedlings grown axenically in vertical Petri dishes. Scale bar: 10 mm. (d) Quantification of lateral root counts in 17-day-old seedlings. Each data point represents an individual seedling; $n = 12$. (e) Quantification of distance from quiescent centre (QC) of root tip to first root hairs. Each data point represents an individual seedling; $n = 9$. (f–h) Representative images of root hairs on the primary root of 7-day-old seedlings grown axenically in vertical Petri dishes. Scale bar: 500 μm . (i) Quantification of root hair length in 7-day-old seedlings in three different regions behind the root tip. Ten individual root hairs at each zone, from each of nine seedlings per genotype were measured; each data point represents the average root hair length in a given zone for a single seedling; $n = 9$ seedlings. (j) Quantification of root hair density at the same three regions behind the root tip. Each data point represents the calculated density for an individual seedling; $n = 9$ seedlings. Black asterisks indicate a significant difference relative to Bd21-3; green asterisks denote a significant difference between *Bdkai2-1* and *Bdkai2-2*; * $P < 0.05$; ** $P < 0.01$; *** $P < 0.001$; **** $P < 0.0001$; ns, not significant (ANOVA).

transcriptional marker of KAI2-dependent activity in several species (Soós et al., 2012; Waters et al., 2012; Végh et al., 2017; Carbonnel et al., 2020b; Sun et al., 2020). We therefore examined transcript levels of the three *Brachypodium* *DLK2* homologues, namely *BdDLK2a*, *BdDLK2b* and *BdDLK2c*, following spore inoculation (Figure 3g–i). All three transcripts were very weakly expressed in roots and could not be quantified reliably in mock-treated samples; however, there was a clear induction of all three transcripts in colonised roots of Bd21-3 that was absent in *Bdkai2-1* and *Bdkai2-2*. In summary, these results demonstrate that KAI2-dependent signalling is a clear necessity for AM colonisation in *Brachypodium*, and most likely a conserved requirement across monocots.

BdKAI2-dependent transcriptional regulation in *Brachypodium*

We used RNA-seq to assess the transcriptional impact of BdKAI2-dependent signalling during the development of *Brachypodium* seedlings. We compared three genotypes

(wild-type Bd21-3, *Bdkai2-1* and *Bdkai2-2*) and four treatments (mock, 1 μM KAR₁, 1 μM KAR₂ and 10 μM *rac*-GR24) with triplicate samples. Treatments were limited to 4 h duration to identify early transcriptional responses.

To identify genes regulated by BdKAI2, we compared mock-treated Bd21-3, *Bdkai2-1* and *Bdkai2-2* transcriptomes. Based on a fold change ≥ 1.5 or ≤ 0.66 and P -value ≤ 0.05 , we found a total of 615 genes that were differentially expressed relative to Bd21-3, of which only 123 (20%) were common to both *Bdkai2* alleles (Figure 4a; Table S3). This result suggests that secondary, unidentified mutations likely contributed to differential gene expression, and underscores the need to examine multiple mutant alleles. We thus defined these 123 genes as 'BdKAI2-specific', while recognising that this analysis will include genes that are mis-regulated as a secondary effect of loss of KAI2 function.

We next identified those genes that were differentially expressed in Bd21-3 seedlings following treatment with karrikins, using the same cut-off criteria as above. We excluded the few genes that were karrikin-responsive in

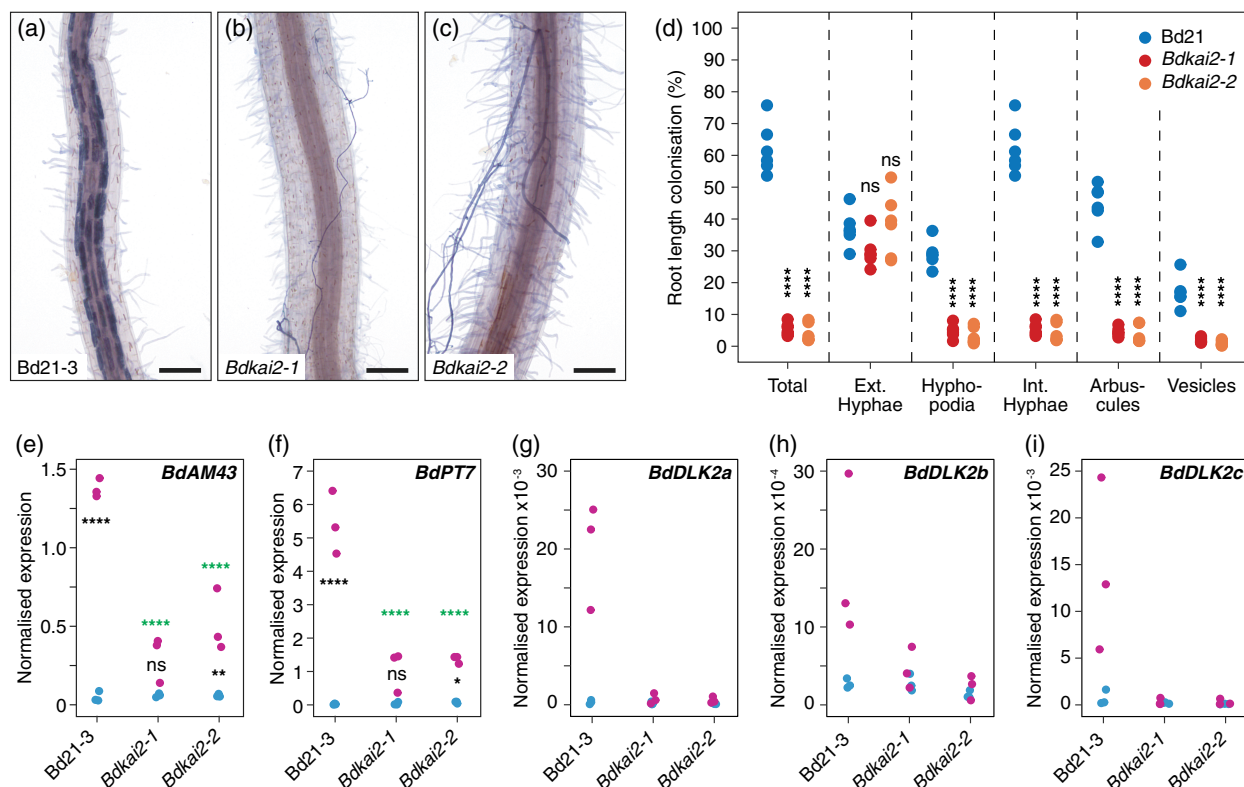


Figure 3. KAI2 is required for root colonisation by arbuscular-mycorrhiza (AM) fungi in *Brachypodium distachyon*. (a–c) Colonisation of wild-type (Bd21-3) and *Bdkai2* roots 6 weeks after inoculation with spores of *Rhizophagus irregularis* as revealed by acid-ink staining. Scale bar: 100 μ m. (d) Stage-specific quantification of root colonisation by *R. irregularis*. Ext., external; Int., internal. Asterisks indicate a significant difference from Bd21-3 for each stage: **** P < 0.0001; ns, not significant (P > 0.05; two-way ANOVA, n = 6 biological replicates). (e, f) Quantification of AM marker transcripts, and (g–i) transcripts corresponding to the three *Brachypodium DLK2* paralogues in roots of seedlings treated with spores of *R. irregularis* (magenta) or mock-treated (blue). Each dot corresponds to a distinct biological replicate comprising roots from two seedlings per genotype. Black asterisks indicate a significant difference between treatments within the same genotype; green asterisks show significant differences between Bd21-3 and each *Bdkai2* allele following treatment with *R. irregularis*: * P < 0.05; ** P < 0.01; *** P < 0.001; **** P < 0.0001; ns, not significant (two-way ANOVA, n = 3 biological replicates). For *BdDLK2a*, *BdDLK2b* and *BdDLK2c*, transcripts could not be consistently detected in the mock-treated condition, so significance tests were not performed.

both *Bdkai2-1* and *Bdkai2-2* (Figure S5; Table S4). Among 197 KAR₁-responsive genes and 239 KAR₂-responsive genes, 119 genes (27%) responded to both KAR₁ and KAR₂ (Figure 4b; Table S5). Thus, the KAR₁ and KAR₂ transcriptomes overlapped, but were also substantially non-congruent. We used a similar process to identify 169 genes responsive to *rac*-GR24 via BdKAI2, and identified a further 159 that were also responsive to KAR₁ and/or KAR₂ (Figure 4b). A core set of 70 genes were responsive to all three ligands via BdKAI2, of which 12 were also among the 123 BdKAI2-specific genes (Table S5). We further identified a subset of 41 transcripts that were differentially regulated in response to *rac*-GR24 in Bd21-3 and both *Bdkai2* mutants (Figure 4c; Table S5). These BdKAI2-independent genes presumably represent BdD14-specific targets; notably, this group included *BdDWARF53* (Figure S6). Differential expression levels from RNA-seq and quantitative reverse transcriptase-polymerase chain reaction (RT-PCR) correlated well (Figure S6; Table S6), suggesting that the RNA-seq data were robust.

We performed hierarchical clustering analysis on 571 genes (Table S7) classified as either BdKAI2-specific, karrikin-specific or *rac*-GR24-specific as defined above. Among the 16 clusters identified, cluster 6 contained genes downregulated by karrikins and *rac*-GR24 in a BdKAI2-dependent manner, while clusters 3, 5 and 9 were characterised by genes that were predominantly upregulated by karrikins and *rac*-GR24 (Figure 4d). Cluster 8 included genes predominantly upregulated by KAR₁, while cluster 2 was typified by *rac*-GR24-specific genes. Perhaps because of the relatively small number of differentially expressed genes (DEGs), or because of their diverse functions, gene enrichment analysis could not define biological or molecular functions to most clusters, with the exception of clusters 2 and 4 (Table S8). Cluster 2 was highly enriched (>100-fold) for glutathione-, oxylipin- and amino acid-related metabolic processes. Cluster 4, which contained a number of BdKAI2-specific genes that tended to be upregulated in *Bdkai2*, was highly enriched (>100-fold) for genes involved in branched-chain amino acid breakdown, and

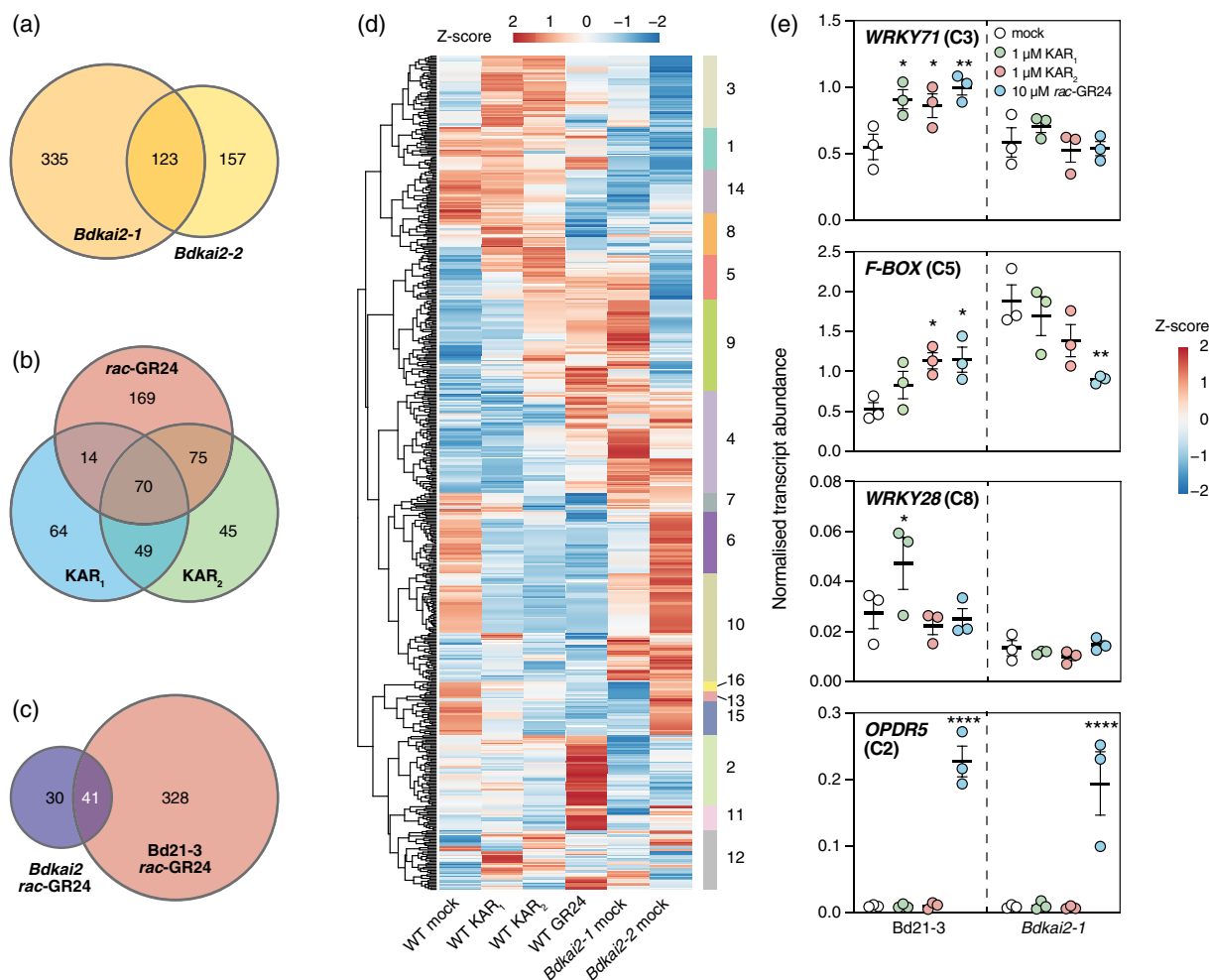


Figure 4. KAI2-dependent and KAI2-independent transcriptome responses in *Brachypodium distachyon*. (a) Overlap of differentially expressed genes (DEGs) in mock-treated *Bdkai2-1* versus mock-treated *Bdkai2-2* seedlings. DEGs were defined by $FC \geq 1.5$, $P < 0.05$. (b) Identification of DEGs specific to treatment with KAR_1 , KAR_2 and *rac-GR24*, and dependent upon BdKAI2. KARRIKIN-specific transcripts are those whose expression responded to KAR_1 or KAR_2 treatments in Bd21-3, but not in both *Bdkai2-1* and *Bdkai2-2*. (c) Identification of 41 putative targets of BdD14, as determined by transcripts induced by *rac-GR24* in all three genotypes (Bd21-3, *Bdkai2-1* and *Bdkai2-2*). (d) Hierarchical clustering analysis of 571 KAR_1 -specific, KAR_2 -specific, *rac-GR24*-specific and BdKAI2-specific DEGs with selection criteria of $FC \geq 1.5$, $P < 0.05$. Blue and red represent downregulation and upregulation of DEGs, respectively. Z-scores were calculated from log-transformed count data. The optimal number of clusters was determined by the gap statistic method (RStudio). Maximum/complete linkage clustering and heatmap drawing were made with RStudio. (e) Abundance of selected transcripts determined by quantitative reverse transcriptase-polymerase chain reaction (RT-PCR). C2, C3, C5 and C8 refer to clusters shown in (d). RNA was extracted from a fully independent experiment in which samples were treated identically to the samples used for RNA-seq. Transcript levels were normalised to *BdUBC18*; n.d., not determinable due to weak expression. Asterisks indicate a significant difference from mock-treated within each genotype: * $P < 0.05$; ** $P < 0.01$; *** $P < 0.001$; **** $P < 0.0001$ (two-way ANOVA, $n = 3$ biological replicates). Gene locus tags are *WRKY71*, Bradi3g06070.1; *F-BOX*, Bradi1g37010.1; *WRKY28*, Bradi1g30870.1; *OPDR5*, Bradi1g05870.1.

moderately enriched (20-fold) for genes relating to organic acid and small molecule metabolism. These gene ontology (GO) terms were similarly represented in a separate analysis of the 123 BdKAI2-specific genes (Table S8). These results suggest that BdKAI2-dependent activity influences specific aspects of carbon and nitrogen metabolism.

Although the 571 DEGs were functionally diverse, a number of similarities to transcriptomic datasets from other species were identified (Table S5). For example, homologues encoding the ethylene biosynthetic enzyme *ACC SYNTHASE* (Bradi5g19100; cluster 5) were also

reported to be KAR_1 -responsive in lettuce (Soós et al., 2012) and Lotus (Carbonnel et al., 2020a) and *kai2* mutant of Arabidopsis (Li et al., 2017). Likewise, *FLAVANONE 3-DIOXYGENASE 2* (Bradi1g77040) was previously reported as a KAI2-related or KAR_1 -responsive transcript in Arabidopsis (Nelson et al., 2010; Li et al., 2017), lettuce (Soós et al., 2012) and Lotus (Carbonnel et al., 2020a). Furthermore, six members of the WRKY transcription factor superfamily were induced by KAR_1 or KAR_2 . Homologues of *WRKY28* (Bradi1g30870), *WRKY31* (Bradi2g08620) and *WRKY71* (Bradi3g06070; all cluster 3) were also

upregulated by KAR₁ in lettuce (Soós et al., 2012) or in a Lotus *kai2a kai2b* mutant (Carbonnel et al., 2020a). We mapped these and other KAI2-implicated homologues onto a phylogeny of WRKY proteins, and found discrete clusters within type IIa and IIb WRKY sub-groups (Figure S7). Tentatively, this result implies that specific WRKY transcription factors might be conserved mediators of KAI2-dependent signalling.

We performed quantitative RT-PCR on a fully independent set of RNA samples to validate selected DEGs of interest. From cluster 3, *WRKY71* was induced approximately 1.5-fold by all three compounds in a KAI2-dependent manner, and an *F-BOX* gene (Bradi1g37010, cluster 5) showed a significant twofold response to KAR₂ and *rac*-GR24 in wild-type (Figure 4e). From cluster 8, *WRKY28* (Bradi1g30870) showed a similar level of induction, but only in response to KAR₁. *rac*-GR24-specific genes (clusters 2 and 11) generally responded much more strongly: *OPDR5* (Bradi1g05870), which encodes a putative 12-oxophytodienoate reductase and thus likely is involved in jasmonate biosynthesis, showed a ~40-fold KAI2-independent induction (Figure 4e), similar as in Lotus (Carbonnel et al., 2020c). These results indicate that the expression changes identified by RNA-seq are experimentally reproducible under our conditions.

BdKAI2 shows enhanced responses to desmethyl butenolides

In the RNA-seq experiment, *BdDLK2c* (Bradi2g14500) responded positively to 1 μ M KAR₂, but *BdDLK2b* did not, and *BdDLK2a* transcripts were not detected. Likewise, we were surprised not to recover the orthologue of *KAR-UP F-BOX1* (*KUF1*; Bradi1g34910), which is KAR₁-responsive and KAI2-dependent in Arabidopsis (Nelson et al., 2010; Waters et al., 2012). To establish whether these transcripts are sensitive to butenolides via BdKAI2, we first examined expression of *BdDLK2b* and *BdKUF1* in Bd21-3 and *Bdkai2-1* seedlings treated with 10 μ M KAR₁, KAR₂ or *rac*-GR24 for 3 days. We reasoned that high ligand concentrations and a prolonged treatment period would maximise the observed response.

Consistent with their orthologues in Arabidopsis, both transcripts were repressed in *Bdkai2-1* relative to wild-type. Levels of both transcripts increased several-fold in response to karrikins in a BdKAI2-dependent manner, revealing a preference for KAR₂ over KAR₁ that is consistent with the hypocotyl elongation assays of Arabidopsis transgenics (Figure 1d). However, neither transcript responded to *rac*-GR24 (Figure 5a). This result suggests that BdKAI2 has a much-reduced preference for GR24 relative to karrikins, or that these two transcripts are not sensitive to GR24 in *Brachypodium*.

To investigate these possibilities, we expressed BdKAI2 in the *Atd14 Atkai2-2* background in which endogenous Arabidopsis responses to GR24 are abolished (Waters

et al., 2015b), thereby isolating BdKAI2 from its native cellular context. Relative to mock-treatment, hypocotyls of seedlings expressing GFP-BdKAI2 were 32% and 64% shorter following treatment with 1 μ M KAR₁ and KAR₂, respectively, but only 34% shorter in response to 1 μ M GR24^{ent-5DS} (Figure 5b). As a further reporter of KAI2 activity, we next examined the relative degradation of GFP-BdKAI2 and GFP-AtKAI2 proteins, in seedlings with matched expression levels (Figure S8), following treatment with karrikins and GR24 (Waters et al., 2015a). After 8 h, levels of GFP-BdKAI2 in KAR₂-treated seedlings were reduced by approximately 80% relative to mock-treated seedlings, whereas GFP-BdKAI2 levels were only very marginally (10%) reduced by treatment with an equivalent concentration of GR24^{ent-5DS} (Figure 5c). In contrast, GFP-AtKAI2 showed an equivalent degradation response to 10 μ M KAR₂ and GR24^{ent-5DS} (Figure 5c). Responses of both proteins to KAR₁ and GR24^{5DS} were negligible, consistent with previous findings (Waters et al., 2015a).

Previously, we showed that KAI2 proteins generally respond more sensitively to desmethyl-GR24^{ent-5DS} (dGR24^{ent-5DS}) than to the methyl-substituted equivalent GR24^{ent-5DS} (Yao et al., 2021). To determine if this holds true for BdKAI2, we compared the ligand responses of purified BdKAI2 and AtKAI2 proteins. Both proteins were expressed and assayed in the form of 6xHIS-SUMO fusion proteins to enhance solubility and yields in *Escherichia coli*. Differential scanning fluorimetry (DSF) reports ligand-induced changes in protein thermal stability based on a change in fluorescence of a hydrophobic dye. In DSF, we found that BdKAI2 was not destabilised in response to GR24^{ent-5DS} even at 400 μ M, whereas AtKAI2 showed responses to 50 μ M GR24^{ent-5DS} and greater (Figure 6a). In contrast, both proteins responded to dGR24^{ent-5DS} at 25 μ M and above. We next examined changes in intrinsic tryptophan fluorescence as a means to infer ligand-binding affinity. Both BdKAI2 and AtKAI2 exhibited a much greater suppression of fluorescence in response to dGR24^{ent-5DS} than to GR24^{ent-5DS} (Figure 6b). For AtKAI2, the estimated ligand-binding affinity (K_d) was some 10-fold greater for dGR24^{ent-5DS} than for GR24^{ent-5DS}, and both proteins had a similar binding affinity for dGR24^{ent-5DS}. However, the response of BdKAI2 to GR24^{ent-5DS} was insufficient to determine the K_d (Figure 6b). We also found that the hydrolytic activity of BdKAI2 and AtKAI2 towards the fluorogenic substrate desmethyl-Yoshimulactone Green (dYLG) followed typical Michaelis–Menten kinetics. Although both enzymes had comparable maximal enzymatic rates, AtKAI2 showed approximately sixfold higher affinity for dYLG than BdKAI2 (Figure 6c), which is consistent with the K_d values obtained from tryptophan fluorescence (Figure 6b). The ligand-binding pockets of AtKAI2 and BdKAI2 are broadly the same in terms of size, shape and composition, at least in contrast to AtD14 (Figure S9).

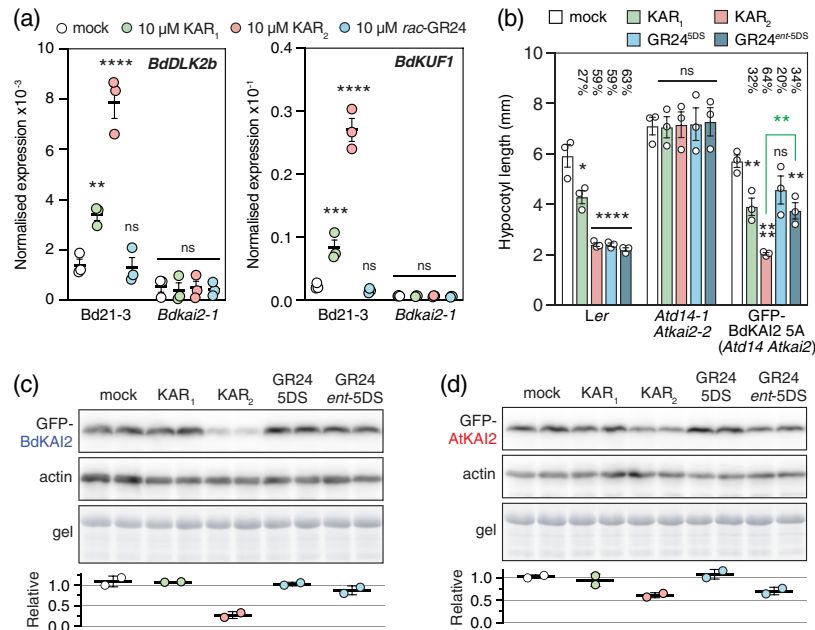


Figure 5. BdKAI2 mediates minimal responses to the strigolactone (SL) analogue GR24. (a) Levels of *BdDLK2b* and *BdKUF1* transcripts in shoots of wild-type *Bd21-3* and *Bdkai2-1* seedlings germinated on nutrient agar plates containing the indicated butenolide compounds. Seedlings were harvested 3 days after germination. Asterisks indicate a significant difference from mock-treated within each genotype: * $P < 0.05$; ** $P < 0.01$; *** $P < 0.001$; **** $P < 0.0001$; ns, not significant (two-way ANOVA, $n = 3$ biological replicates). Error bars indicate SE. (b) Hypocotyl elongation responses of *Arabidopsis* seedlings expressing *AtKAI2pro: GFP-BdKAI2 5A* in the *At14 Atkai2-2* background treated with 1 μ M of the indicated compound. Significance levels as per (a); two-way ANOVA, $n = 3$ experimental replicates of 15–20 seedlings per replicate. Percentages indicate reduction in length relative to mock-treated seedlings of the same genotype. Green asterisks represent outcome of an unpaired *t*-test. Error bars indicate SE. (c, d) Degradation of GFP-BdKAI2 or GFP-AtKAI2 in response to karrikins and GR24. Seedlings expressing either GFP-BdKAI2 (c) or GFP-AtKAI2 (d) under control of the *AtKAI2* promoter and in the *Atkai2-2* background were treated in duplicate with the indicated butenolide at 10 μ M for 8 h. Soluble protein extracts were subjected to immunoblot analysis first with anti-GFP antibodies, and then with anti-actin antibodies as a loading control. Levels of GFP fusion proteins were normalised to actin and then expressed relative to the mock-treated control. Each dot represents one of the two replicates for each treatment, and bars indicate the mean \pm SE.

However, two of the 17 residues that define the pocket surface differ between AtKAI2 and BdKAI2, and conceivably these may contribute to their dissimilar affinities for dYLG (Figure S9). Nevertheless, BdKAI2 showed negligible activity towards the methyl-substituted SL analogue YLG, consistent with previous findings for other KAI2 proteins (Yao et al., 2018, 2021). Altogether, these results indicate that BdKAI2 is intrinsically hyposensitive to GR24 compared with AtKAI2, and instead shows the strong preference for desmethyl butenolides typical of KAI2.

Finally, to examine BdKAI2 substrate preferences *in vivo*, we compared the effect of *KAR*₂, *rac*-GR24 and *rac*-dGR24 on BdKAI2-dependent transcript levels in *Brachypodium* seedlings over a 4-h treatment period, as per our RNA-seq experiments. Under these conditions, *BdDLK2b* and *BdDLK2c* were both induced by GR24 and dGR24, indicating that these transcripts indeed respond to these compounds in *Brachypodium* (Figure 6d). For both *BdDLK2b* and *BdDLK2c*, there was no significant difference in the magnitude of response to GR24 and dGR24 in *Bd21-3*. However, *Bdkai2-1* responded to GR24, implying that some proportion of the response to GR24 observed in *Bd21-3* was independent of BdKAI2, and most probably due to

signalling via BdD14. Accordingly, it is likely that dGR24 is indeed more active via BdKAI2 than GR24 in *Brachypodium*. Meanwhile, *BdKUF1* transcripts were repressed in *Bdkai2-1*, but did not respond to any of the three compounds tested (Figure 6d). Given that *BdKUF1* does respond to karrikins over 3 days (Figure 5a), this result indicates that *BdKUF1* responds much more slowly to butenolides than *BdDLK2b* and *BdDLK2c*.

DISCUSSION

KAI2-dependent signalling influences numerous aspects of plant growth and development, many of which have previously only been inferred from the analysis of a single species. By studying the function of KAI2 in *Brachypodium*, we have identified a number of conserved developmental functions in shoot and root development. Across monocots and dicots, KAI2 is likely involved in leaf morphogenesis and responses to light, root system development, and AM symbiosis. In turn, this emphasises the technical opportunities for modifying plant growth and performance in a wide range of species by modulating KAI2 activity.

We have identified two missense alleles of KAI2, each affected by a glycine replacement. Glycine 56 is an

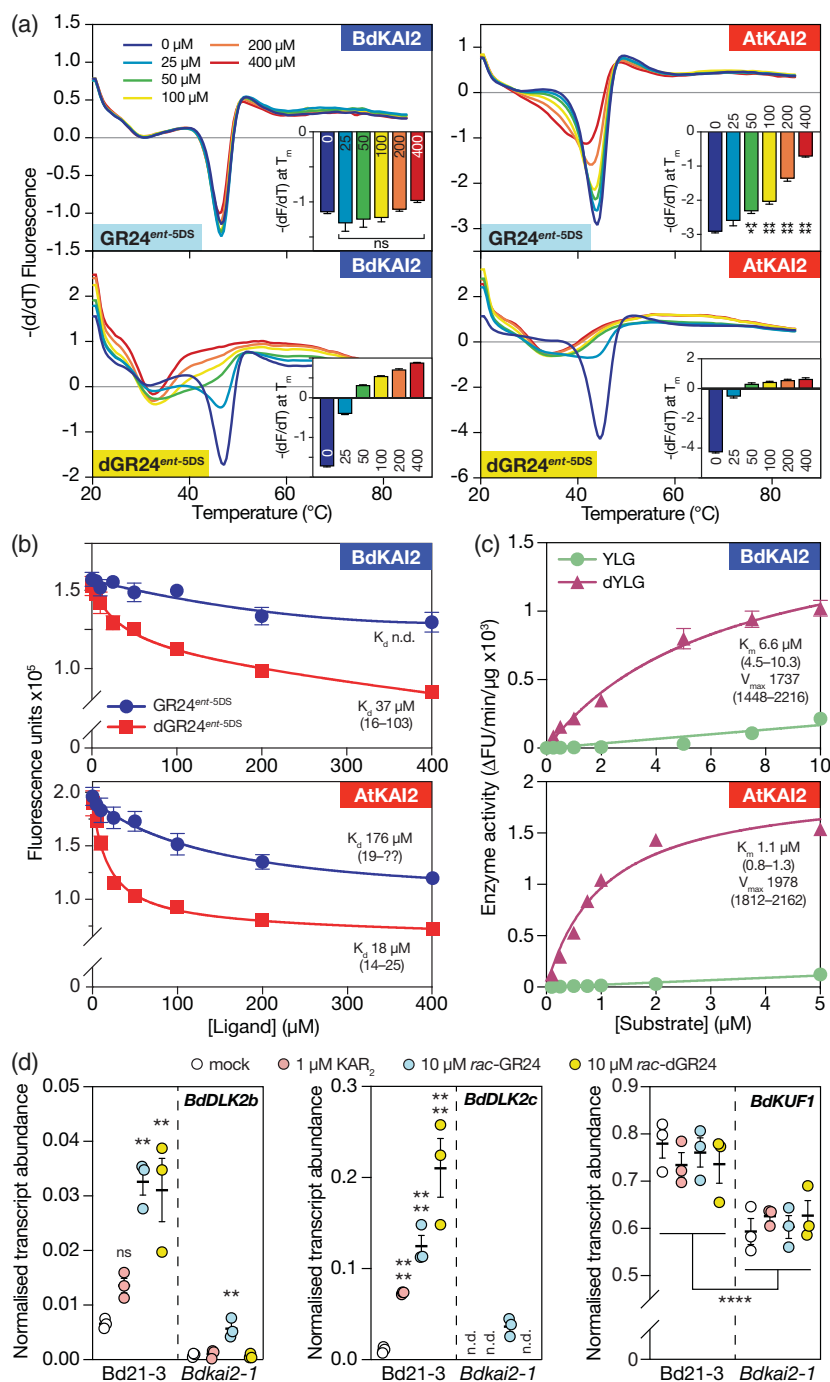


Figure 6. Bdkai2 responds preferentially to desmethyl butenolides. (a) Differential scanning fluorimetry (DSF) assays of SUMO-tagged Bdkai2 (left panels) or Atkai2 (right panels) in response to 0–400 μM GR24^{ent-5DS} (upper panels) or desmethyl-GR24^{ent-5DS} (lower panels). Each curve is the average of three sets of reactions, each comprising four technical replicates. Insets plot the minimum value of $-(dF/dT)$ at the melting point of the protein as determined in the absence of ligand (means \pm SE, $n = 3$). (b) Quenching of intrinsic tryptophan fluorescence of purified SUMO-tagged Bdkai2 and Atkai2 proteins in response to increasing concentrations of GR24^{ent-5DS} or dGR24^{ent-5DS}. Dissociation constants (K_d) were estimated by non-linear regression; numbers in parentheses indicate 95% confidence intervals; n.d., not determinable; ??, no upper bound. Data are means \pm SE of four technical replicates. (c) Hydrolysis of the profluorescent butenolides YLG and desmethyl-YLG (dYLG) by Bdkai2 (upper panel) and Atkai2 (lower panel). Data are means \pm SE of four technical replicates; error bars smaller than the symbol are not shown. Estimates of V_{max} and K_d for dYLG data are shown with 95% confidence intervals in parentheses. Parameters were not determinable for YLG data. (d) Levels of *BdDLK2b*, *BdDLK2c* and *BdKUF1* transcripts in shoots of wild-type Bd21-3 and *Bdkai2-1* seedlings treated with the indicated butenolide compounds for 4 h. Transcript levels were normalised to *BdUBC18*; n.d., not determinable due to weak expression. Asterisks indicate a significant difference from mock-treated within each genotype, or between groups as indicated: * $P < 0.05$; ** $P < 0.01$; *** $P < 0.001$; **** $P < 0.0001$; ns, $P > 0.05$ (two-way ANOVA, $n = 3$ biological replicates).

absolutely conserved residue among homologues of both KAI2 and D14, and is the dominant residue at the corresponding position in DLK2 (Figure S2a). In contrast, although glycine 54 is highly conserved among KAI2 proteins, it is universally a cysteine residue in D14 and predominantly a phenylalanine in DLK2. In AtKAI2 and AtD14, both residues are located below the cap domain on a short loop that is highly similar in topology in both proteins (Figure S2b). Along with the cap domain, this loop forms part

of the interface with D3 (the rice orthologue of MAX2) following activation of AtD14 by GR24 (Figure S2c; Yao et al., 2016). Cys55 and Gly57 of AtD14 – which are structurally correspondent to Gly54 and Gly56 of AtKAI2 – form part of a hydrogen bond network that likely contributes substantially to the AtD14-D3 interaction (Figure S2d; Yao et al., 2016). Assuming that KAI2 interacts with the F-box protein in a similar manner to D14, then the functional implications of the G56D and G54D substitutions are clear.

Interestingly, DLK2 and related proteins in seed plants have lost many of the residues associated with MAX2 interaction, suggesting that DLK2 likely does not have a similar function as a receptor (Bythell-Douglas et al., 2017). The lack of conservation of Gly56 in DLK2, and the stability of BdKAI2^{G56D}, further suggest that this residue does not have a purely structural role for this type of α/β -hydrolase, but instead is crucial for the interaction with MAX2. More puzzling, however, is the functional relevance of the strict conservation of glycine versus cysteine at position 54/55 in KAI2 versus D14.

Although most roles of KAI2 are conserved between *Brachypodium* and *Arabidopsis*, unexpectedly we found that *Brachypodium kai2* mutants show a comparatively modest increase in the rate of water loss from leaves. This subtle phenotype was only discernible in the stronger of the two mutant alleles, and required a relatively large experimental sample size to detect. The drought-sensitive *Arabidopsis kai2* phenotype results from increased cuticle permeability, as well as impaired ability to regulate stomatal aperture (Li et al., 2017). The plant cuticle is composed of an electron-dense layer of a lipid biopolymer called cutin, which is covered by a 'cuticle proper' rich in aliphatic wax components (Yeats and Rose, 2013). It is this cuticle proper that is lacking in *Atkai2*, which is reflected by down-regulation of numerous genes involved in cuticle formation and wax biosynthesis, such as *ECERIFERUM1* and *ECERIFERUM4* (Li et al., 2017). Intriguingly, we found that *ECERIFERUM3* (Bradi1g31140) was karrikin-inducible in *Brachypodium*, as were *3-KETOACYL-CoA SYNTHASE6* (*KCS6*; Bradi1g44020) and *KCS12* (Bradi3g55040). All three of these genes encode enzymes responsible for very-long-chain fatty acid biosynthesis and, therefore, for normal cuticle formation (Millar et al., 1999; Haslam et al., 2015). Thus, in both species, cuticular wax biosynthesis appears, at least in part, to be under KAI2-dependent control. Why, then, the different water loss phenotypes? First, although wax biosynthesis genes may be karrikin-inducible in *Brachypodium*, basal levels of expression may be adequate for cuticle formation in *Bdkai2* mutants. Second, *Brachypodium* appears to have a more substantial cuticle than *Arabidopsis*. Estimates of total cuticular wax levels from intact *Arabidopsis* leaves range from 0.7 to 0.9 $\mu\text{g cm}^{-1}$, based on chloroform extraction (Kosma et al., 2009; Buschhaus and Jetter 2012; Vráblová et al., 2020), whereas *Brachypodium* leaves contain 1–4 $\mu\text{g cm}^{-1}$, with higher levels at earlier growth stages (Wang et al., 2018b). Finally, inherent differences in wax composition between species may also account for differential effects of KAI2 upon the cuticle: for example, *Arabidopsis* leaf wax contains 30% fatty acids and ~25% primary alcohols (Buschhaus and Jetter, 2012), while *Brachypodium* leaf wax contains only 1–3% fatty acids and over 80% primary alcohols (Wang et al., 2018b). Given that a role for KAI2 in

drought tolerance has been assessed in only these two divergent species, it will be important to establish the causative nature of its effect on the cuticle, and to what degree this function is taxonomically restricted.

We found that the KAR₁ and KAR₂ transcriptomes of *Brachypodium* were overlapping but substantially distinct. Superficially, this could imply that, in *Brachypodium*, there are alternate modes of KAI2-dependent signal transduction via different downstream SMXLs, which in turn could regulate different transcriptional targets. However, there is no SMAX1 paralogue in *Brachypodium* that could perform such a function with KAI2 (Moturu et al., 2018). In *Arabidopsis*, where SMXL2 is partially redundant to SMAX1 (Stanga et al., 2016), there is no evidence that each paralogue regulates different targets. We are also unaware of any other transcriptomic study directly comparing the effects of KAR₁ and KAR₂, and so distinct responses may not be unique to *Brachypodium*. Most probably, we have documented the effects of measuring transcript levels at a single time point following treatment with two different compounds. KAR-responsive transcripts differ in their induction kinetics in *Arabidopsis* (Nelson et al., 2010), which we also found for *BdDLK2b/c* and *BdKUF1*. It is clear that BdKAI2, like AtKAI2, is more efficiently activated by KAR₂ than KAR₁ (Figures 1d and 5a,c), and by desmethyl butenolides in general (Figure 6). Perhaps then, at 4 h post-treatment, we observed a mixture of 'early' responding transcripts for KAR₁, and 'late' responding transcripts for KAR₂. Indeed, many transcripts classified as KAR₂-specific were responsive to KAR₁, but marginally missed the cut-off criteria (Table S5). The reasons behind differential activation of KAI2 by KAR₁ and KAR₂ include desmethyl ligand preference, but also growing evidence in support of karrikins undergoing metabolic activation prior to interaction with KAI2 (Waters et al., 2015b; Khosla et al., 2020; Wang et al., 2020; Yao et al., 2021). Under this scenario, KAR₁ and KAR₂ might be activated at different rates.

In our transcriptome dataset, six members of the WRKY transcription factor family were upregulated by karrikins. WRKY transcription factors can either repress or activate gene expression related to a vast array of plant developmental processes, including seed development and germination, senescence, abscisic acid (ABA) signalling and response to biotic and abiotic stress stimuli (Rushton et al., 2010). The closest *Arabidopsis* homologue of *BdWRKY53* is *AtWRKY46*, which contributes to osmotic/salt stress-dependent lateral root inhibition via regulation of ABA signalling and auxin homeostasis (Ding et al., 2015). Close homologues of *BdWRKY31* are thought to mediate ABA sensitivity in *Malus domestica* (Zhao et al., 2019) and leaf senescence in *Arabidopsis* (Niu et al., 2020). The two *BdWRKY24* genes are close homologues of the pathogen-responsive *AtWRKY33*, while the structurally similar *BdWRKY28* and *BdWRKY71* are

phylogenetically related to *AtWRKY18*, *40* and *60* (Figure S7). These latter three WRKYs are also pathogen-induced, physically interact with each other, and have a partially redundant, mixed effect on salicylic acid- and jasmonic acid-mediated defence responses (Xu et al., 2006). Furthermore, *AtWRKY18* and *40*, along with *AtWRKY33* form an important functional hub within a WRKY regulatory circuitry to target key components of microbe- and damage-associated molecular pattern perception and signalling (Birkenbihl et al., 2017). *KAI2* has been implicated in modulating responses to salt and osmotic stress in *Arabidopsis* (Wang et al., 2018a), and *KAR₁* was shown to ameliorate the damaging effects of *Pseudomonas aeruginosa* on *Arabidopsis* and lettuce leaves (Mandabi et al., 2014). We speculate that karrikin signalling modulates abiotic and biotic stress responses via WRKY-dependent transcriptional networks.

Plants clearly have the capacity to regulate AM symbiosis because high levels of soil phosphate result in low rates of root colonisation due to inactivity of the central transcriptional regulator of phosphate starvation responses *PHR2* (Balzergue et al., 2010; Breuillin et al., 2010; Das et al., 2021; Shi et al., 2021). It is likely that *KAI2* has a conserved role in this regulation, because *KAI2* is essential for AM symbiosis in rice, *Petunia* and now *Brachypodium*. We observed that, similar to the *d14l* (i.e. *kai2*) mutant of rice (Gutjahr et al., 2015), when exposed to a strong inoculum the fungus can enter the root, albeit at extremely low frequency. Thereafter all stages of colonisation, including structurally normal arbuscules, can be formed in the absence of *KAI2* (Figure 3). This suggests that the initiation of root colonisation is blocked, but there is no strict block on progression of colonisation once it is initiated. *KAI2*-dependent signalling may condition the root into a state permissive for fungal colonisation (Hull et al., 2021) by reducing *SMAX1* levels and thereby increasing expression of SL biosynthesis and the common symbiosis genes (Choi et al., 2020). This may boost hyphopodium formation and symbiotic commitment of the plant host. Furthermore, *KAI2*-dependent signalling may have a role in regulating the lifespan of AM symbiosis, at least on the level of individual arbuscules. Recently, an AM-inducible *DLK2* homologue was shown to constrain mycorrhizal colonisation and control the life cycle of arbuscules in tomato (Ho-Plágaro et al., 2021). In *Brachypodium*, all three *DLK2* homologues were induced by AM colonisation, as were *DLK2a* (Os05g51240) and *DLK2b* (Os01g41240) in rice (Kobae et al., 2018). It is thus reasonable to speculate that *DLK2* has a conserved role as a negative regulator of AM colonisation, at least in seed plants. The fact that *DLK2* expression is *KAI2*-dependent further indicates that *DLK2* might act in a negative feedback loop to place a limit upon the extent of AM symbiosis. Speculatively, this loop could form one mechanism by which nutrient status could

influence the permissive condition of the root, if, for example, *DLK2* and *KAI2* activity were responsive to phosphate (Das et al., 2021; Villaécija-Aguilar et al., 2021). Mechanistically it is not obvious how this might work; as mentioned above, *DLK2* is unlikely to operate as a receptor in the same manner as *KAI2* or *D14*. However, *DLK2* from *Arabidopsis* retains hydrolytic activity towards butenolides (Végh et al., 2017). Future molecular-genetic analyses of *DLK2* homologues from mycorrhizal species will be key to solving this enigma.

EXPERIMENTAL PROCEDURES

Plant material and growth conditions

Arabidopsis thaliana ecotype *Ler* and *Brachypodium distachyon* Bd21-3 were used as wild-types. *Atkai2-2*, *Atd14-1*, *Atd14 Atkai2* and *35S:AtKAI2* (all *Ler*) were described previously (Waters et al., 2012, 2015b; Waters and Smith, 2013). *AtKAI2pro:GFP-BdKAI2*, *AtKAI2pro:GFP-Bdkai2^{G56D}* and *AtKAI2pro:GFP-AtKAI2* constructs were transformed into the *Atkai2-2* mutant via floral dipping. *AtKAI2pro:GFP-BdKAI2* 5A was later crossed with *Atd14 Atkai2*.

The *Bdkai2-1* mutation (G56D) was isolated from a sodium-azide-mutagenised population screened using a TILLING procedure (Dalmais et al., 2013), except that the mutations were detected by NGS (Methods S1). The *Bdkai2-2* mutation (line NaN1793) was identified from a high-throughput bulk sequencing screen of mutagenised populations (Granier et al., 2016). Homozygous mutants were confirmed by genomic PCR (Figure S1; see primers in Table S1).

Plants were grown in peat-based compost (Seedling Substrate Plus; Bord Na Mona, Ireland), vermiculite and perlite mixed in a 6:1:1 ratio. *Arabidopsis* was grown under long-day conditions (16 h day/8 h night) or short-day conditions (8 h/16 h), at 22°C day/18°C night and 60% relative humidity. Light was provided by broad-spectrum white LED panels or fluorescent tubes at 120–150 $\mu\text{mol photons m}^{-2} \text{sec}^{-1}$. *Brachypodium* was grown under the same long-day conditions for phenotypic analysis but, when grown for seed production, light intensity was 250 $\mu\text{mol photons m}^{-2} \text{sec}^{-1}$.

To synchronise germination, *Brachypodium* seeds were soaked in water for 3 h, and then the glume was removed by the awn using forceps. Seeds were surface sterilised with a 30-sec rinse in 70% ethanol, a 3-min rinse in 10% sodium hypochlorite, and four brief rinses with sterile distilled water. Seeds were transferred onto two layers of water-saturated Whatman paper, and the dish sealed with gas-permeable tape. Seeds were stratified for 3 days in the dark at 4°C.

Seed germination assays

Arabidopsis seed germination assays were performed using triplicate batches of seed as described previously (Sun et al., 2020). For *Brachypodium*, we found that seed germination of intact seeds was low (<10%) and non-synchronous on soil, nutrient agar or saturated filter paper, and was not enhanced by pre-imbibition, addition of karrikins or by cold stratification. We found that physical removal of the awn from imbibed seeds was sufficient to induce synchronous germination of ~100% of seeds, irrespective of genotype, within 2 days of transfer to growth conditions described above (data not shown).

Hypocotyl elongation assays

Hypocotyl elongation assays were performed as described previously (Sun et al., 2020), except that red light was provided at 20 $\mu\text{mol photons m}^{-2} \text{sec}^{-1}$.

Water loss measurements

Plants were grown in a randomised position in individual 8-cm pots in trays for 4 weeks under long-day conditions. The aerial parts were detached in order of position in the tray, placed on a plastic weighing boat and weighed on scales to three decimal places. The material was placed in a laminar flow hood at ambient temperature (approximately 22°C) and weighed, in the same randomised order from the tray, at hourly intervals. Water loss was defined as the change in mass relative to initial mass.

Chlorophyll measurements

Arabidopsis was grown under short-day conditions, randomised across multiple trays. Five, 0.8-cm² leaf punches were taken from rosette leaves 8, 9 and 10 from a single 4-week-old plant, and pooled to make one sample. For *Brachypodium*, the leaf blades of an entire 4-week-old seedling grown in a randomised position under long-day conditions were defined as a single sample. Total chlorophyll was extracted in 80% ethanol and quantified as previously described (Lolle et al., 1997) using a FLUOstar Omega microplate reader (BMG Labtech).

Quantification of root phenotypes

Stratified *Brachypodium* seeds were transferred to half-strength MS medium (pH 5.8) and 1.5% (w/v) agar, and grown under long-day conditions. Roots were imaged with a Zeiss Discovery V8 microscope and AxioCam 503 colour camera. For *Brachypodium*, the length of 10 root hairs at 3–4 mm, 5–6 mm and 7–8 mm behind the root tip of 7-day-old seedlings were averaged. Root hair density was approximated by thresholding the image (Figure S10). Seventeen-day-old plants were used for lateral root analysis.

For Arabidopsis, the roots of 5-day-old seedlings were examined. The length of 10 root hairs per plant between 2 and 3 mm distance from the root tip were averaged. Root hair density was defined as root hair count between 2 and 3 mm behind the root tip.

AM colonisation in *Brachypodium*

Seeds were germinated on Whatman paper under long-day conditions at 24°C with fluorescent lamps emitting 500 $\mu\text{mol photons m}^{-2} \text{sec}^{-1}$. Ten days after germination, two seedlings per pot were transferred to 9-cm pots containing quartz sand, watered twice a week with deionised water and fertilised once a week with half-strength Hoagland solution containing 25 μM phosphate. Each pot was inoculated with 1000 spores of AM fungus *Rhizophagus irregularis* (Agronutrition, Toulouse, France). The whole root system was harvested 6 weeks post-inoculation. AM fungi were stained and colonisation quantified as described (Torabi et al., 2021). Roots were visualised with a DM6B microscope and DFC9000GT camera (Leica, Wetzlar, Germany).

Leaf morphometric analysis

Leaf image acquisition and analysis were performed with LeafAnalyser (Weight et al., 2008) and ImageJ (<https://imagej.nih.gov/ij/>) as described previously (Scaffidi et al., 2013). Leaves 8, 9 and

10, of 5–8 plants per genotype, were analysed from 40-day-old Arabidopsis grown under short-day conditions.

Treatment of seedlings for transcript analysis

Stratified *Brachypodium* seeds were transferred to 0.5 \times MS medium (pH 5.9) and 0.8% (w/v) agar, and incubated under long-day conditions for 3 days. For Figure 5(a), butenolide treatments were added to the medium at the time of pouring; one biological replicate consisted of a pool of about 10 seedlings. For Figures 4(e) and 6(d), approximately 10, 3-day-old *Brachypodium* seedlings per replicate were transferred to 25 ml liquid 0.5 \times MS medium in 250-ml Erlenmeyer flasks, and treated with butenolides 24 h later, as described previously (Sun et al., 2020). Prior to RNA extraction, shoots were separated from roots. For Figure 3(e–i), root tissue from two seedlings per replicate was harvested 6 weeks after inoculation with *R. irregularis* spores.

RNA extraction, DNase treatment and cDNA synthesis were performed as described previously (Waters et al., 2015b). Quantitative RT-PCR was performed either on a Bio-Rad CFX384 Touch system with qPCR GreenMaster highROX (Jena Bioscience, Jena, Germany; Figure 3), ABI 7500 Fast real-time PCR System with ABI Fast SYBR Green Master Mix (ThermoFisher Scientific, Waltham, MA, USA; Figure S6; Table S6), or Roche Lightcycler 480 instrument with Luna Universal qPCR master mix (New England Biolabs, Ipswich, MA, USA; all other figures).

Transcriptome analysis

Seedlings were transferred to 250-ml Erlenmeyer flasks and treated with butenolides for 4 h as described above. RNA was extracted from shoot tissue and DNase I-treated. RNA integrity scores ≥ 7 were confirmed with an Agilent 2200 TapeStation. Paired-end libraries were prepared using the TruSeq RNA Library Prep Kit v2 (Illumina, San Diego, CA, USA). Sequencing was performed on an Illumina NextSeq 550 instrument with a NextSeq 500/550 High Output Kit v2.5 (300 cycles) to generate 2 \times 150 nt reads. Adapter trimming, read mapping onto the *B. distachyon* Bd21v.3.1 reference genome and read counts were carried out with CLC Genomics Workbench 11.0. Differential expression analysis was performed using EdgeR (Robinson et al., 2010). Venn diagrams were generated using the Venn plug-in of the OriginPro (2018) software. Maximum/complete linkage clustering (R package: stats/hclust), heatmap drawing (R package: NMF/heatmap) and cluster optimisation using the gap statistic method (R package: cluster/clusGap) were accomplished in RStudio (<http://www.rstudio.com>). The Panther classification system (<http://pantherdb.org/>) was used to analyse GO term enrichment on each identified cluster separately (Thomas et al., 2003).

KAI2 degradation assay and immunoblotting

KAI2 degradation assays in Arabidopsis seedlings were performed as described previously (Waters et al., 2015a). Total soluble protein was extracted, electrophoresed, blotted and probed with anti-GFP (ThermoFisher A11122) and anti-actin (Sigma A0480) antibodies as described previously (Sun et al., 2020). Chemiluminescence signals were quantified by densitometry using ImageJ (<https://imagej.nih.gov/ij/>).

Protein expression and purification

SUMO-tagged fusion proteins were expressed in *E. coli* Rosetta DE3 pLysS cells (Merck-Millipore, Burlington, MA, USA). Procedures for expression and purification were described previously (Sun et al., 2020).

DSF, intrinsic tryptophan fluorescence and hydrolysis assays

The DSF was performed and analysed as described previously (Sun et al., 2020), as were ITF and hydrolysis assays with YLG and dYLG (Yao et al., 2021).

Statistical analysis

Data were analysed using one- or two-way ANOVA ($\alpha = 0.05$, with Tukey's multiple comparisons test) or Kruskal–Wallis *H*-test. Prior to ANOVA, germination data were arcsine-transformed. Statistical tests were implemented in Graphpad Prism v9.1.

ACKNOWLEDGEMENTS

The authors gratefully acknowledge funding support from an Australian Research Council Future Fellowship (FT150100162) and a fellowship support grant from the University of Western Australia to MTW. YM was a recipient of a joint PhD scholarship from the China Scholarship Council. VS received funding from the Hungarian National Research, Development and Innovation Office (NKFIH Grants K128644 and GINOP-2.3.2-15-2016-00029). CG received funding from the Emmy Noether Program (GU1423/1-1) of the Deutsche Forschungsgemeinschaft (DFG), and KV a doctoral student fellowship from the German Academic Exchange Service (DAAD). The work conducted by the US DOE Joint Genome Institute is supported by the Office of Science of the US Department of Energy under Contract no. DE-AC02-05CH11231. The authors thank Adrian Scaffidi and Gavin Flematti (UWA) for chemical synthesis, and Gergely Maróti (Biological Research Centre, Szeged, Hungary) and Seqomics Ltd (Mórahalom, Hungary) for Illumina sequencing and basic bioinformatics analysis. The TILLING work was supported by INRAE and the LabEx Saclay Plant Sciences - SPS (ANR-10-LABX-40-SPS). Open Access funding enabled and organized by Projekt DEAL.

AUTHOR CONTRIBUTIONS

YM, KV, NI, EB, VS, MK, SFD, LO and MTW conducted experiments. KM, MD, AB, RS, JV and DLC provided *Brachypodium* mutant seeds and screened mutant populations. NI and VS performed transcriptomic analysis and curated data. VS, CG and MTW conceived the study, analysed data and provided supervision. MTW prepared figures. MTW, VS and YM wrote the article with contributions from all authors.

CONFLICT OF INTEREST

The authors declare no competing interests.

DATA AVAILABILITY STATEMENT

RNA-seq data are available from the NCBI Gene Expression Omnibus under accession number GSE174000. All other data that support the findings of this study are available from the corresponding author upon reasonable request.

SUPPORTING INFORMATION

Additional Supporting Information may be found in the online version of this article.

Figure S1. Molecular confirmation of *Bdkai2-1* and *Bdkai2-2* alleles.

Figure S2. Conservation and functional significance of residues 54 and 56 in KAI2, D14 and DLK2 proteins.

Figure S3. *Brachypodium* KAI2 complements the *Arabidopsis kai2-2* seed germination and leaf shape phenotypes.

Figure S4. *Brachypodium* KAI2 complements the *Arabidopsis kai2-2* root hair phenotype.

Figure S5. Genes responding to karrikins in a BdKAI2-independent manner.

Figure S6. Technical validation of RNA-seq results via qRT-PCR.

Figure S7. Phylogenetic tree of WRKY proteins from *Brachypodium distachyon*, *Arabidopsis thaliana*, *Oryza sativa* var. *japonica*, *Hordeum vulgare*, *Lotus japonicus* and *Lactuca sativa*.

Figure S8. Matching expression levels of GFP-AtKAI2 and GFP-BdKAI2 in transgenic *Arabidopsis*.

Figure S9. Comparison of predicted ligand-binding pockets of AtKAI2, BdKAI2 and AtD14.

Figure S10. Methodology for measuring root hair length and density in *Brachypodium distachyon*.

Methods S1. Molecular cloning and TILLING screen for *Bdkai2-1* alleles.

Table S1. List of oligonucleotides used in this study

Table S2. Analysis of *Bdkai2* mutations with PROVEAN and Meta-SNP

Table S3. List of 123 BdKAI2-specific genes

Table S4. List of DEGs in response to KAR₁, KAR₂ and *rac*-GR24

Table S5. Karrikin- and *rac*-GR24-responsive genes in *Bdkai2-1* and *Bdkai2-2*

Table S6. List of genes and samples used for RNA-seq validation

Table S7. Hierarchical clustering analysis on BdKAI2-specific, karrikin-specific or *rac*-GR24-specific DEGs

Table S8. Gene ontology analysis of DEGs following hierarchical clustering

REFERENCES

- Arellano-Saab, A., Bunsick, M., Galib, H.A., Zhao, W., Schuetz, S., Bradley, J.M. et al. (2021) Three mutations repurpose a plant karrikin receptor to a strigolactone receptor. *Proceedings of the National Academy of Sciences of the United States of America*, **118**, e2103175118.
- Balzergue, C., Puech-Pagès, V., Bécard, G. & Rochange, S.F. (2010) The regulation of arbuscular mycorrhizal symbiosis by phosphate in pea involves early and systemic signalling events. *Journal of Experimental Botany*, **62**, 1049–1060.
- Bennett, T., Liang, Y., Seale, M., Ward, S., Müller, D. & Leyser, O. (2016) Strigolactone regulates shoot development through a core signalling pathway. *Biology Open*, **5**, bio.021402.
- Birkenbihl, R.P., Kracher, B., Roccaro, M. & Somssich, I.E. (2017) Induced genome-wide binding of three *Arabidopsis* WRKY transcription factors during early MAMP-triggered immunity. *Plant Cell*, **29**, 20–38.
- Breullin, F., Schramm, J., Hajirezaei, M., Ahkami, A., Favre, P., Druge, U. et al. (2010) Phosphate systemically inhibits development of arbuscular mycorrhiza in *Petunia hybrida* and represses genes involved in mycorrhizal functioning. *The Plant Journal*, **64**, 1002–1017.
- Brutnell, T.P., Bennetzen, J.L. & Vogel, J.P. (2012) *Brachypodium distachyon* and *Setaria viridis*: model genetic systems for the grasses. *Annual Review of Plant Biology*, **66**, 1–21.
- Bürger, M. & Chory, J. (2020) The many models of strigolactone signaling. *Trends in Plant Science*, **25**, 395–405.
- Buschhaus, C. & Jetter, R. (2012) Composition and physiological function of the wax layers coating *Arabidopsis* leaves: β -amyirin negatively affects the intracuticular water barrier. *Plant Physiology*, **160**, 1120–1129.
- Bythell-Douglas, R., Rothfels, C.J., Stevenson, D.W.D., Graham, S.W., Wong, G.K.-S., Nelson, D.C. et al. (2017) Evolution of strigolactone receptors by gradual neo-functionalization of KAI2 paralogues. *BMC Biology*, **15**, 52.

- Capriotti, E., Altman, R.B. & Bromberg, Y. (2013) Collective judgment predicts disease-associated single nucleotide variants. *BMC Genomics*, **14**, S2.
- Carbonnel, S., Das, D., Varshney, K., Kolodziej, M.C., Villaécija-Aguilar, J.A. & Gutjahr, C. (2020a) The karrikin signaling regulator SMAX1 controls *Lotus japonicus* root and root hair development by suppressing ethylene biosynthesis. *Proceedings of the National Academy of Sciences of the United States of America*, **117**, 21757–21765.
- Carbonnel, S., Torabi, S., Griesmann, M., Bleek, E., Tang, Y., Buchka, S. *et al.* (2020b) *Lotus japonicus* karrikin receptors display divergent ligand-binding specificities and organ-dependent redundancy. *PLoS Genetics*, **16**, e1009249.
- Carbonnel, S., Torabi, S. & Gutjahr, C. (2020c) MAX2-independent transcriptional responses to rac-GR24 in *Lotus japonicus* roots. *Plant Signaling & Behavior*, **16**, 1840852.
- Choi, Y. & Chan, A.P. (2015) PROVEAN web server: a tool to predict the functional effect of amino acid substitutions and indels. *Bioinformatics*, **31**, 2745–2747.
- Choi, J., Lee, T., Cho, J., Servante, E., Pucker, B., Summers, W. *et al.* (2020) The negative regulator SMAX1 controls mycorrhizal symbiosis and strigolactone biosynthesis in rice. *Nature Communications*, **11**, 2114.
- Conn, C.E. & Nelson, D.C. (2016) Evidence that KARRIKIN-INSENSITIVE2 (kai2) receptors may perceive an unknown signal that is not karrikin or strigolactone. *Frontiers in Plant Science*, **6**, 1219.
- Dalmais, M., Antelme, S., Ho-Yue-Kuang, S., Wang, Y., Darracq, O., Bouvier d'Yvoire, M. *et al.* (2013) A TILLING platform for functional genomics in *Brachypodium distachyon*. *PLoS One*, **8**, e65503.
- Das, D., Paries, M., Hobecker, K., Gigl, M., Dawid, C., Lam, H.-M. *et al.* (2021) PHOSPHATE STARVATION RESPONSE transcription factors enable arbuscular mycorrhiza symbiosis. *Nature Communications*, In press. <https://doi.org/10.1038/s41467-022-27976-8>.
- Ding, Z.J., Yan, J.Y., Li, C.X., Li, G.X., Wu, Y.R. & Zheng, S.J. (2015) Transcription factor WRKY46 modulates the development of Arabidopsis lateral roots in osmotic/salt stress conditions via regulation of ABA signaling and auxin homeostasis. *The Plant Journal*, **84**, 56–69.
- Flematti, G.R., Ghisalberti, E.L., Dixon, K.W. & Trengove, R.D. (2004) A compound from smoke that promotes seed germination. *Science*, **305**, 977–977.
- Flematti, G.R., Ghisalberti, E.L., Dixon, K.W. & Trengove, R.D. (2009) Identification of alkyl substituted 2H-Furo[2,3-c]pyran-2-ones as germination stimulants present in smoke. *Journal of Agricultural and Food Chemistry*, **57**, 9475–9480.
- Girin, T., David, L.C., Chardin, C., Sibout, R., Krapp, A., Ferrario-Méry, S. *et al.* (2014) *Brachypodium*: a promising hub between model species and cereals. *Journal of Experimental Botany*, **65**, 5683–5696.
- Granier, F., Lemaire, A., Wang, Y., LeBris, P., Antelme, S., Vogel, J. *et al.* (2016) Genetics and genomics of *Brachypodium*. In: *Plant genetics and genomics: crops and models*. Cham: Springer International Publishing, pp. 155–170. https://doi.org/10.1007/7397_2015_20
- Guo, Y., Zheng, Z., Clair, J.J.L., Chory, J. & Noel, J.P. (2013) Smoke-derived karrikin perception by the α/β -hydrolase KAI2 from Arabidopsis. *Proceedings of the National Academy of Sciences of the United States of America*, **110**, 8284–8289.
- Gutjahr, C., Gobbato, E., Choi, J., Riemann, M., Johnston, M.G., Summers, W. *et al.* (2015) Rice perception of symbiotic arbuscular mycorrhizal fungi requires the karrikin receptor complex. *Science*, **350**, 1521–1524.
- Hamiaux, C., Drummond, R.S.M., Janssen, B.J., Ledger, S.E., Cooney, J.M., Newcomb, R.D. *et al.* (2012) DAD2 is an α/β hydrolase likely to be involved in the perception of the plant branching hormone, strigolactone. *Current Biology*, **22**, 2032–2036.
- Haslam, T.M., Haslam, R., Thoraval, D., Pascal, S., Delude, C., Domergue, F. *et al.* (2015) ECERIFERUM2-LIKE proteins have unique biochemical and physiological functions in very-long-chain fatty acid elongation. *Plant Physiology*, **167**, 682–692.
- Hong, J.J., Park, Y.-S., Bravo, A., Bhattarai, K.K., Daniels, D.A. & Harrison, M.J. (2012) Diversity of morphology and function in arbuscular mycorrhizal symbioses in *Brachypodium distachyon*. *Planta*, **236**, 851–865.
- Ho-Plágaro, T., Morcillo, R.J.L., Tamayo-Navarrete, M.I., Huertas, R., Molinero-Rosales, N., López-Ráez, J.A. *et al.* (2021) DLK2 regulates arbuscule hyphal branching during arbuscular mycorrhizal symbiosis. *The New Phytologist*, **229**, 548–562.
- Hull, R., Choi, J. & Paszkowski, U. (2021) Conditioning plants for arbuscular mycorrhizal symbiosis through DWARF14-LIKE signalling. *Current Opinion in Plant Biology*, **62**, 102071.
- Jiang, L., Liu, X., Xiong, G., Huihui, L., Chen, F., Wang, L. *et al.* (2013) DWARF 53 acts as a repressor of strigolactone signalling in rice. *Nature*, **504**, 401.
- Keymer, A. & Gutjahr, C. (2018) Cross-kingdom lipid transfer in arbuscular mycorrhiza symbiosis and beyond. *Current Opinion in Plant Biology*, **44**, 137–144.
- Khosla, A., Morffy, N., Li, Q., Faure, L., Chang, S.H., Yao, J. *et al.* (2020) Structure–function analysis of SMAX1 reveals domains that mediate its karrikin-induced proteolysis and interaction with the receptor KAI2. *Plant Cell*, **32**, 2639–2659.
- Kobae, Y., Kameoka, H., Sugimura, Y., Saito, K., Ohtomo, R., Fujiwara, T. *et al.* (2018) Strigolactone biosynthesis genes of rice are required for the punctual entry of arbuscular mycorrhizal fungi into the roots. *Plant & Cell Physiology*, **59**, 544–553.
- Kosma, D.K., Bourdenx, B., Bernard, A., Parsons, E.P., Lü, S., Joubès, J. *et al.* (2009) The impact of water deficiency on leaf cuticle lipids of Arabidopsis. *Plant Physiology*, **151**, 1918–1929.
- Lee, I., Kim, K., Lee, S., Lee, S., Hwang, E., Shin, K. *et al.* (2018) Functional analysis of a missense allele of KARRIKIN-INSENSITIVE2 that impairs ligand-binding and downstream signaling in *Arabidopsis thaliana*. *Journal of Experimental Botany*, **69**, 3609–3623.
- Li, W., Nguyen, K.H., Chu, H.D., Ha, C.V., Watanabe, Y., Osakabe, Y., Leyva-González, M.A. *et al.* (2017) The karrikin receptor KAI2 promotes drought resistance in Arabidopsis thaliana. *PLoS Genetics*, **13**, e1007076.
- Liu, G., Stirnemann, M., Gübeli, C., Egloff, S., Courty, P.-E., Aubry, S. *et al.* (2019) Strigolactones play an important role in shaping exodermal morphology via a KAI2-dependent pathway. *iScience*, **17**, 144–154.
- Lolle, S.J., Berlyn, G.P., Engstrom, E.M., Krolkowski, K.A., Reiter, W.-D. & Pruitt, R.E. (1997) Developmental regulation of cell interactions in the Arabidopsis fiddlehead-1 mutant: a role for the epidermal cell wall and cuticle. *Developmental Biology*, **189**, 311–321.
- Mandabi, A., Ganin, H., Krief, P., Rayo, J. & Meijler, M.M. (2014) Karrikins from plant smoke modulate bacterial quorum sensing. *Chemical Communications*, **50**, 5322–5325.
- Millar, A.A., Clemens, S., Zachgo, S., Giblin, E.M., Taylor, D.C. & Kunst, L. (1999) CUT1, an Arabidopsis gene required for cuticular wax biosynthesis and pollen fertility, encodes a very-long-chain fatty acid condensing enzyme. *Plant Cell*, **11**, 825–838.
- Moturu, T.R., Thula, S.K., Singh, R.K., Nodzyski, T., Vareková, R.S., Friml, J. *et al.* (2018) Molecular evolution and diversification of SMAX-like gene family. *Journal of Experimental Botany*, **69**, 2367–2378.
- Mur, L.A.J., Allainguillaume, J., Catalán, P., Hasterok, R., Jenkins, G., Lesniewska, K. *et al.* (2011) Exploiting the *Brachypodium* Tool Box in cereal and grass research. *The New Phytologist*, **191**, 334–347.
- Nelson, D.C., Riseborough, J.-A., Flematti, G.R., Stevens, J., Ghisalberti, E.L., Dixon, K.W. *et al.* (2009) Karrikins discovered in smoke trigger Arabidopsis seed germination by a mechanism requiring gibberellic acid synthesis and light. *Plant Physiology*, **149**, 863–873.
- Nelson, D.C., Flematti, G.R., Riseborough, J.-A., Ghisalberti, E.L., Dixon, K.W. & Smith, S.M. (2010) Karrikins enhance light responses during germination and seedling development in *Arabidopsis thaliana*. *Proceedings of the National Academy of Sciences of the United States of America*, **107**, 7095–7100.
- Nelson, D.C., Scaffidi, A., Dun, E.A., Waters, M.T., Flematti, G.R., Dixon, K.W. *et al.* (2011) F-box protein MAX2 has dual roles in karrikin and strigolactone signaling in *Arabidopsis thaliana*. *Proceedings of the National Academy of Sciences of the United States of America*, **108**, 8897–8902.
- Niu, F., Cui, X., Zhao, P., Sun, M., Yang, B., Deyholos, M.K. *et al.* (2020) WRKY42 transcription factor positively regulates leaf senescence through modulating SA and ROS synthesis in *Arabidopsis thaliana*. *The Plant Journal*, **104**, 171–184.
- Robinson, M.D., McCarthy, D.J. & Smyth, G.K. (2010) edgeR: a Bioconductor package for differential expression analysis of digital gene expression data. *Bioinformatics*, **26**, 139–140.
- Roth, R. & Paszkowski, U. (2017) Plant carbon nourishment of arbuscular mycorrhizal fungi. *Current Opinion in Plant Biology*, **39**, 50–56.
- Rushton, P.J., Somssich, I.E., Ringler, P. & Shen, Q.J. (2010) WRKY transcription factors. *Trends in Plant Science*, **15**, 247–258.

- de Saint Germain, A., Clavé, G., Badet-Denisot, M.A. *et al.* (2016) An histidine covalent receptor and butenolide complex mediates strigolactone perception. *Nature Chemical Biology*, **12**, 787–794.
- Scaffidi, A., Waters, M.T., Ghisalberti, E.L., Dixon, K.W., Flematti, G.R. & Smith, S.M. (2013) Carlactone-independent seedling morphogenesis in *Arabidopsis*. *The Plant Journal*, **76**, 1–9.
- Scaffidi, A., Waters, M.T., Sun, Y.K., Skelton, B.W., Dixon, K.W., Ghisalberti, E.L. *et al.* (2014) Strigolactone hormones and their stereoisomers signal through two related receptor proteins to induce different physiological responses in *Arabidopsis*. *Plant Physiology*, **165**, 1221–1232.
- Shabek, N., Tichiarelli, F., Mao, H., Hinds, T.R., Leyser, O. & Zheng, N. (2018) Structural plasticity of D3–D14 ubiquitin ligase in strigolactone signalling. *Nature*, **563**, 652–656.
- Shi, J., Zhao, B., Zheng, S., Zhang, X., Wang, X., Dong, W. *et al.* (2021) A phosphate starvation response-centered network regulates mycorrhizal symbiosis. *Cell*, **184**, 5527–5540.e18.
- Smith, S.E. & Smith, F.A. (2011) Roles of arbuscular mycorrhizas in plant nutrition and growth: New paradigms from cellular to ecosystem scales. *Plant Biology*, **62**, 227–250.
- Soós, V., Sebestyén, E., Posta, M., Kohout, L., Light, M.E., Staden, J. *et al.* (2012) Molecular aspects of the antagonistic interaction of smoke-derived butenolides on the germination process of Grand Rapids lettuce (*Lactuca sativa*) achenes. *The New Phytologist*, **196**, 1060–1073.
- Soundappan, I., Bennett, T., Morffy, N., Liang, Y., Stanga, J.P., Abbas, A. *et al.* (2015) SMAX1-LIKE/D53 family members enable distinct MAX2-dependent responses to strigolactones and karrikins in *Arabidopsis*. *Plant Cell*, **27**, 3143–3159.
- Stanga, J.P., Smith, S.M., Briggs, W.R. & Nelson, D.C. (2013) SUPPRESSOR OF MORE AXILLARY GROWTH2 1 controls seed germination and seedling development in *Arabidopsis*. *Plant Physiology*, **163**, 318–330.
- Stanga, J.P., Morffy, N. & Nelson, D.C. (2016) Functional redundancy in the control of seedling growth by the karrikin signaling pathway. *Planta*, **243**, 1397–1406.
- Stevens, J.C., Merritt, D.J., Flematti, G.R., Ghisalberti, E.L. & Dixon, K.W. (2007) Seed germination of agricultural weeds is promoted by the butenolide 3-methyl-2H-furo[2,3-c]pyran-2-one under laboratory and field conditions. *Plant and Soil*, **298**, 113–124.
- Sun, X.-D. & Ni, M. (2011) HYPOSENSITIVE TO LIGHT, an alpha/beta fold protein, acts downstream of ELONGATED HYPOCOTYL 5 to regulate seedling de-etiolation. *Molecular Plant*, **4**, 116–126.
- Sun, Y.K., Flematti, G.R., Smith, S.M. & Waters, M.T. (2016) Reporter gene-facilitated detection of compounds in *Arabidopsis* leaf extracts that activate the karrikin signaling pathway. *Frontiers in Plant Science*, **7**, 1799.
- Sun, Y.K., Yao, J., Scaffidi, A., Melville, K.T., Davies, S.F., Bond, C.S. *et al.* (2020) Divergent receptor proteins confer responses to different karrikins in two ephemeral weeds. *Nature Communications*, **11**, 1264.
- Swarbreck, S.M., Guerringue, Y., Matthus, E., Jamieson, F.J.C. & Davies, J.M. (2019) Impairment in karrikin but not strigolactone sensing enhances root skewing in *Arabidopsis thaliana*. *The Plant Journal*, **98**, 607–621.
- Swarbreck, S.M., Mohammad-Sidik, A. & Davies, J.M. (2020) Common components of the strigolactone and karrikin signaling pathways suppress root branching in *Arabidopsis thaliana*. *Plant Physiology*, **184**, 18–22.
- The International Brachypodium Initiative. (2010) Genome sequencing and analysis of the model grass *Brachypodium distachyon*. *Nature*, **463**, 763–768.
- Thomas, P.D., Campbell, M.J., Kejarawal, A., Mi, H., Karlak, B., Daverman, R. *et al.* (2003) PANTHER: a library of protein families and subfamilies indexed by function. *Genome Research*, **13**, 2129–2141.
- Torabi, S., Varshney, K., Villaécija-Aguilar, J.A., Keymer, A. & Gutjahr, C. (2021) Strigolactones, methods and protocols. *Methods in Molecular Biology*, **2309**, 157–177.
- Végh, A., Incze, N., Fábrián, A., Huo, H., Bradford, K.J., Balázs, E. *et al.* (2017) Comprehensive analysis of DWARF14-LIKE2 (DLK2) reveals its functional divergence from strigolactone-related paralogs. *Frontiers in Plant Science*, **8**, 1641.
- Villaécija-Aguilar, J.A., Hamon-Josse, M., Carbonnel, S., Kretschmar, A., Schmidt, C., Dawid, C. *et al.* (2019) SMAX1/SMXL2 regulate root and root hair development downstream of KAI2-mediated signalling in *Arabidopsis*. *PLoS Genetics*, **15**, e1008327.
- Villaécija-Aguilar, J.A., Kőrösy, C., Maisch, L., Hamon-Josse, M., Petrich, A., Magosch, S. *et al.* (2021) KAI2 promotes *Arabidopsis* root hair elongation at low external phosphate by controlling local accumulation of AUX1 and PIN2. *Current Biology*, **32**, 228–236.e3. <https://doi.org/10.1016/j.cub.2021.10.044>
- Vráblová, M., Vrábl, D., Sokolová, B., Marková, D. & Hronková, M. (2020) A modified method for enzymatic isolation of and subsequent wax extraction from *Arabidopsis thaliana* leaf cuticle. *Plant Methods*, **16**, 129.
- Wang, L., Wang, B., Jiang, L., Liu, X., Li, X., Lu, Z. *et al.* (2015) Strigolactone signaling in *Arabidopsis* regulates shoot development by targeting D53-like SMXL repressor proteins for ubiquitination and degradation. *Plant Cell*, **27**, 3128–3142.
- Wang, L., Waters, M.T. & Smith, S.M. (2018a) Karrikin-KAI2 signalling provides *Arabidopsis* seeds with tolerance to abiotic stress and inhibits germination under conditions unfavourable to seedling establishment. *The New Phytologist*, **219**, 605–618.
- Wang, Y., Sun, Y., You, Q., Luo, W., Wang, C., Zhao, S. *et al.* (2018b) Three fatty acyl-coenzyme A reductases, BdfAR1, BdfAR 2 and BdfAR 3, are involved in cuticular wax primary alcohol biosynthesis in *Brachypodium distachyon*. *Plant & Cell Physiology*, **59**, 527–543.
- Wang, L., Xu, Q., Yu, H., Ma, H., Li, X., Yang, J. *et al.* (2020) Strigolactone and karrikin signaling pathways elicit ubiquitination and proteolysis of SMXL2 to regulate hypocotyl elongation in *Arabidopsis thaliana*. *Plant Cell*, **32**, 2251–2270.
- Waters, M.T. & Smith, S.M. (2013) KAI2- and MAX2-mediated responses to karrikins and strigolactones are largely independent of HY5 in *Arabidopsis* seedlings. *Molecular Plant*, **6**, 63–75.
- Waters, M.T., Nelson, D.C., Scaffidi, A., Flematti, G.R., Sun, Y.K., Dixon, K.W. *et al.* (2012) Specialisation within the DWARF14 protein family confers distinct responses to karrikins and strigolactones in *Arabidopsis*. *Development*, **139**, 1285–1295.
- Waters, M.T., Scaffidi, A., Flematti, G. & Smith, S.M. (2015a) Substrate-induced degradation of the α/β -fold hydrolase KARRIKIN INSENSITIVE2 requires a functional catalytic triad but is independent of MAX2. *Molecular Plant*, **8**, 814–817.
- Waters, M.T., Scaffidi, A., Moulin, S.L.Y., Sun, Y.K., Flematti, G.R. & Smith, S.M. (2015b) A *Selaginella moellendorffii* ortholog of KARRIKIN INSENSITIVE2 functions in *Arabidopsis* development but cannot mediate responses to karrikins or strigolactones. *Plant Cell*, **27**, 1925–1944.
- Waters, M.T., Gutjahr, C., Bennett, T. & Nelson, D.C. (2017) Strigolactone signaling and evolution. *Annual Review of Plant Biology*, **68**, 1–31.
- Weight, C., Parnham, D. & Waites, R. (2008) LeafAnalyser: a computational method for rapid and large-scale analyses of leaf shape variation. *The Plant Journal*, **53**, 578–586.
- Xu, X., Chen, C., Fan, B. & Chen, Z. (2006) Physical and functional interactions between pathogen-induced *Arabidopsis* WRKY18, WRKY40, and WRKY60 transcription factors. *Plant Cell Online*, **18**, 1310–1326.
- Yao, R., Ming, Z., Yan, L., Li, S., Wang, F., Ma, S. *et al.* (2016) DWARF14 is a non-canonical hormone receptor for strigolactone. *Nature*, **536**, 469.
- Yao, J., Mashiguchi, K., Scaffidi, A., Akatsu, T., Melville, K.T., Morita, R. *et al.* (2018) An allelic series at the KARRIKIN INSENSITIVE 2 locus of *Arabidopsis thaliana* decouples ligand hydrolysis and receptor degradation from downstream signalling. *The Plant Journal*, **96**, 75–89.
- Yao, J., Scaffidi, A., Meng, Y., Melville, K.T., Komatsu, A., Khosla, A. *et al.* (2021) Desmethyl butenolides are optimal ligands for karrikin receptor proteins. *The New Phytologist*, **230**, 1003–1016.
- Yeats, T.H. & Rose, J.K.C. (2013) The formation and function of plant cuticles. *Plant Physiology*, **163**, 5–20.
- Zhao, L.-H., Zhou, X.E., Yi, W., Wu, Z., Liu, Y., Kang, Y. *et al.* (2015) Destabilization of strigolactone receptor DWARF14 by binding of ligand and E3-ligase signaling effector DWARF3. *Cell Research*, **25**, 1219.
- Zhao, X.-Y., Qi, C.-H., Jiang, H., You, C.-X., Guan, Q.-M., Ma, F.-W. *et al.* (2019) The MdWRKY31 transcription factor binds to the MdRAV1 promoter to mediate ABA sensitivity. *Horticulture Research*, **6**, 66.
- Zheng, J., Hong, K., Zeng, L., Wang, L., Kang, S., Qu, M. *et al.* (2020) Karrikin signaling acts parallel to and additively with strigolactone signaling to regulate rice mesocotyl elongation in darkness. *Plant Cell*, **32**, 2780–2805.
- Zhou, F., Lin, Q., Zhu, L., Ren, Y., Zhou, K., Shabek, N. *et al.* (2013) D14-SCFD3-dependent degradation of D53 regulates strigolactone signalling. *Nature*, **504**, 406.